



## Variations in extracellular vesicle shedding of *Cystoisospora suis* stages (Apicomplexa: Coccidia)



Anna Sophia Feix<sup>a,\*</sup>, Astrid Laimer-Digruber<sup>b</sup>, Teresa Cruz-Bustos<sup>a</sup>, Gerhard Steiner<sup>c</sup>, Bärbel Ruttkowski<sup>a</sup>, Monika Ehling-Schulz<sup>b</sup>, Anja Joachim<sup>a</sup>

<sup>a</sup>Institute of Parasitology, Department for Biological Sciences and Pathobiology, University of Veterinary Medicine Vienna, Veterinärplatz 1 A-1210 Vienna, Austria

<sup>b</sup>Institute of Microbiology, Department for Biological Sciences and Pathobiology, University of Veterinary Medicine, Veterinärplatz 1 A-1210 Vienna, Austria

<sup>c</sup>Department of Integrative Zoology, Faculty of Life Sciences, University of Vienna, Djerassiplatz 1 1030 Vienna, Austria

### ARTICLE INFO

#### Article history:

Received 12 June 2024

Received in revised form 21 November 2024

Accepted 5 January 2025

Available online 8 January 2025

#### Keywords:

*Isoospora suis*

Apicomplexa

Ectosomes

Microvesicles

Sexual development

Host-parasite interaction

### ABSTRACT

*Cystoisospora suis*, a porcine enteral parasite of the order Coccidia, is characterized by a complex life cycle, with asexual and sexual development in the epithelium of the host gut and an environmental phase as an oocyst. All developmental stages vary greatly in their morphology and function, and therefore excrete different bioactive molecules for intercellular communication. Due to their complex development, we hypothesized that the extracellular vesicles (EVs) cargo is highly dependent on the life cycle stages from which they are released. This study aimed to characterize and compare EVs of all developmental stages of *C. suis*. Nanoparticle tracking analysis and microscopy were used to determine particle numbers and size distributions of stage-specific parasite EVs. Furthermore, Fourier-transform infrared spectral analysis was employed for the metabolic fingerprinting of EVs, and the lipid and protein profiles of all parasite stages were determined. Overall, the study revealed that asexual, sexual and transmissible stages of *C. suis* release different EVs during the parasite's life cycle. EVs of endogenous asexual and sexual stages were found to be more similar to each other than to those of the transmissible environmental stage, the oocyst. Furthermore, the ratio of fatty acids to polysaccharides and proteins changed during parasite development. In particular, proteins associated with the Apicomplexa and those involved in vesicle shedding showed changes in expression in all parasite stages. Lipid analysis showed that fatty acids were found in the same concentration through all parasite stages, whereas the amount of sterolipids, sphingolipids and glycerolipids changed between the parasite stages. In conclusion, this study, which presents the first known characterization of *C. suis* EVs, demonstrates a link between EVs and the respective developmental stages of the parasite, and putative functions in the parasite-parasite and host-parasite interplays.

© 2025 The Author(s). Published by Elsevier Ltd on behalf of Australian Society for Parasitology. This is an open access article under the CC BY license (<http://creativecommons.org/licenses/by/4.0/>).

## 1. Introduction

Extracellular vesicles (EVs) are membranous structures formed by all cells during biological processes and are generally classified in three major types – exosomes, ectosomes and apoptotic bodies – based on their size, biogenesis and composition (Ofir-Birin and Regev-Rudzki, 2019; Nik and Shahidan, 2020). Exosomes are 30–100 nm in size, of endocytic origin and are released after the fusion of multivesicular bodies with the plasma membrane (Raposo and Stoorvogel, 2013). Ectosomes are more heterogeneous in shape, can be larger (0.1–1 µm in diameter) and are shed directly from the plasma membrane (Hugel et al., 2005). Consequently, different

EVs can transport different cargos for putative intercellular communication purposes. Until very recently, EVs have been regarded as a by-product of cellular metabolism; however, there is increasing evidence that they play decisive roles as mediators in the transmission of biological signals and immune responses (Isaac et al., 2021; Fridman et al., 2022).

In protozoa, secretion of EVs can occur directly from the parasite's organellar compartments and through parasite-infected or antigen-stimulated host cells in response to in vitro and in vivo physiological stressors (Olajide and Cai, 2020). They are also considered to be important communication tools between parasite cells, as well as between parasite and host, facilitating parasite growth by modifying the activity of the targeted host tissue (Drurey and Maizels, 2021). For this, lipid-bound structures are important, and it is suggested that the most effective means of delivery for these lipids as a communication tool is via EVs

\* Corresponding author.

E-mail address: [Anna.Feix@vetmeduni.ac.at](mailto:Anna.Feix@vetmeduni.ac.at) (A.S. Feix).

(Coakley et al., 2016, 2017). Furthermore, the usual lipid bi-membranous layer of EVs varies in some protozoans, e.g. *Leishmania major* promastigote exosomes have their content protected by a phospholipid membrane (Leitherer et al., 2017). Increasingly, evidence of the release of EVs by protozoan parasites shows that they act both in parasite–parasite communication and in host–parasite interactions.

The phylum Apicomplexa comprises more than 5,000 species, including protozoan genera of significant veterinary and human medical importance – *Plasmodium*, *Babesia*, *Cryptosporidium*, *Cystoisospora*, *Cyclospora*, *Sarcocystis* and *Toxoplasma* (Marcilla et al., 2014). Current knowledge on EVs in apicomplexan parasites can be summarized as follows: i) studies of the host exosome demonstrated that it contains host as well as parasite proteins (Nawaz et al., 2019); ii) EV proteins are able to modulate the host's immune response (Montaner et al., 2014); iii) novel technical applications for EV analyses can also be used for parasite EVs (Khosravi et al., 2020; Liangsupree et al., 2021). Although previous studies reported on EV release in *Plasmodium* (Ketprasit et al., 2020; Toda et al., 2020), *Toxoplasma* (Ramírez-Flores et al., 2019; Quiarim et al., 2021) and *Neospora* (Lv et al., 2010), these earlier studies did not follow the current MISEV guidelines (Minimal Information for Studies of Extracellular Vesicles, published by the International Society of Extracellular Vesicles; Théry et al., 2018; Witwer et al., 2021; Welsh et al., 2024), therefore comparative analyses of apicomplexan EVs are not possible.

The apicomplexan *Cystoisospora suis* (Biester and Murray, 1934, Studies in infectious enteritis of Swine. 12th International Veterinary Congress, pp. 207–219) is an obligate intracellular protozoan parasite of the order Coccidia (Barta et al., 2005). Its lifecycle is completed within a single host which can be affected by severe diarrhoea and reduced weight gain. Porcine cystoisosporosis (coccidiosis) occurs almost exclusively in suckling piglets and can considerably impair animal health (Joachim and Shrestha, 2019; Lindsay, 2019). Although *C. suis* is usually not considered as a model organism for coccidia (in contrast to its close relative, *Toxoplasma gondii*), an in vitro cultivation system supporting the entire lifecycle in porcine intestinal epithelial cells (IPEC) was established and is continuously improved (Worliczek et al., 2009; Feix et al., 2020). This system permits detailed studies of the parasite's biology, cellular dynamics and host–parasite interactions. In addition, stage-specific gene transcription and translation, developmental changes in protein composition and developmental bottlenecks with reduced numbers of vital stages as putative targets for novel control options can be analysed (Feix et al., 2023).

The environmental stages (oocysts) of *C. suis* contain a sporont with a peripherally located nucleus, which after nuclear division forms two sporocysts containing four sporozoites each. Sporozoites are the actual infectious cellular entities of *C. suis* and are released during the gastrointestinal passage once the oocysts are ingested by the host. Free sporozoites are highly motile and will penetrate the porcine intestine epithelial cells by invagination of the host cell plasma membrane (Pinckney et al., 1993). Within the host cell, sporozoites undergo cellular division by merogony, which results in the formation of motile, crescent-shaped merozoites (Matuschka and Heydorn, 1980; Worliczek et al., 2009; Lindsay et al., 2014). Merozoites released from host cells will reinvade further host cells in a defined number of cycles and finally convert to sexual stages – some will become microgamonts and others macrogamonts. A microgamont undergoes multiple nuclear divisions, which results in the formation of numerous microgametes (Supplementary Fig. S1). The nucleus of a macrogamont, in contrast, does not divide (Scholtyssek and Hammond, 1970; Smith et al., 2002; Feix et al., 2020). It is assumed that a macrogamete is fertilized by a single microgamete to form a zygote, which then

forms a new oocyst (Scholtyssek and Hammond, 1970; Walker et al., 2013; Feix et al., 2020).

We hypothesized that the asexual stages of *C. suis*, which are primarily proliferative to maximize parasite cell numbers, produce distinct EVs compared with the sexual stages, which focus on finding partner cells to form a zygote and progress in development. To test this hypothesis, the study aimed to develop an EV isolation protocol for *C. suis* that aligns with MISEV guidelines, and provide an initial characterization of EVs from different developmental stages of *C. suis* by comparing the morphology, particle profile, and cargo of EVs from asexual, sexual, and environmental stages.

## 2. Materials and methods

### 2.1. *Cystoisospora suis* oocyst collection *ex vivo*

*Cystoisospora suis* oocysts (strain Wien 1) were collected from experimentally infected suckling piglets on the fifth day after infection, cleaned, sporulated in vitro and stored for later use at the Institute of Parasitology, University of Veterinary Medicine Vienna, Austria, as previously described (Worliczek et al., 2007; Feix et al., 2020).

### 2.2. Parasite in vitro cultivation

The in vitro culture system for *C. suis* available at the Institute of Parasitology, University of Veterinary Medicine Vienna, Austria, extends the development time to a 2 week period (compared with 6–7 days in vivo) for improved delineation and harvest of the different life cycle stages (Feix et al., 2020). Intestinal porcine epithelial cells (IPEC-1, ACC 705, Leibniz Institute DSMZ-German Collection of Microorganisms and Cell Cultures GmbH, Leibniz, Germany) were used as host cells for in vitro cultivation of *C. suis*. Cells were seeded in a density of  $4 \times 10^5$  cells per well in a 6-well plate (VWR, Vienna, Austria) and cultured in a DMEM/Ham's F-12 medium (Gibco, Fisher Scientific GmbH, Schwerte, Germany) with 5% FCS (Gibco Thermo Fisher Scientific, Waltham, USA) and 100 U/ml of penicillin and 0.1 mg/ml of streptomycin (PAN BioTech GmbH, Aidenbach, Germany). Cells were infected with  $0.5 \times 10^3$  sporozoites/well released from encysted oocysts and incubated at 40 °C in 5% CO<sub>2</sub> (Feix et al., 2020).

### 2.3. Isolation of EVs at different time points in parasite development

*Cystoisospora suis* stages were obtained on day of cultivation (doc) 6 (asexual stages), doc 10 (sexual stages) and doc 13 (oocysts), and morphologically identified in accordance with Feix et al. (2020). Total medium pooled from all 6-well plates (60 ml) of all infected cells was pooled and centrifuged at 300 g for 5 min. The pellet with the host cells was discarded. In the next centrifugation step, parasites were pelleted at 2000 g for 10 min, after which the parasites were washed with fresh PBS (Thermo Fisher Scientific Inc., Waltham, USA) at 6000 g for 10 min. The cleaned parasites were then incubated for 2 h in fresh (EV-free, FCS-free) DMEM/Ham's F-12 medium (Gibco, Fisher Scientific GmbH, Schwerte, Germany) at 40 °C. After incubation the parasites were separated from their EVs with a sterile 0.22 µm Rotilabo® filter (Carl Roth, Karlsruhe, Germany). EVs were harvested by several ultracentrifugation steps in an Optima TLX centrifuge (Beckman Coulter GmbH, Wien, Austria), first at 124,500 g for 1 h at 4 °C with an MLA-50 fixed-angle rotor to exclude potential large protein aggregates, followed by an EV pellet washing step at 188,700 g for 1 h at 4 °C in a TLA-55 rotor and final EV collection (at the same settings) and resuspension in PBS. Vesicles were harvested after 2 h of incubation, which was determined as the ideal timepoint in a pilot

experiment. The detailed characterization of EVs was performed according to MISEV guidelines (Théry et al., 2018; Witwer et al., 2021).

#### 2.4. Nanoparticle tracking analysis

The effective diameter and size distribution of EVs were measured using the ZetaView × 30 TWIN Laser System 488/640 (Particle Metrix, Inning am Ammersee, Germany) as described previously (Mehdiani et al., 2015; Bachurski et al., 2019) and calibrated using 100 nm polystyrene beads. EVs were diluted 1:1,000 in sterile-filtered H<sub>2</sub>O. Particle tracking analysis was performed in scatter mode with a 488 nm laser with the following settings: minimum brightness 30; minimum area 10; maximum brightness 255; maximum area 1000; temperature 25 °C; shutter of 70 and repeated on three biological replicates with three technical replicates each. Statistical analysis and figure generation have been performed with Graph Pad Prism 8 (GraphPad Software, San Diego, CA, USA).

#### 2.5. Transmission electron microscopy (TEM)

For transmission electron microscopy (TEM) imaging, both pelleted EVs and pelleted parasites with EVs were fixed in 4% neutral buffered glutaraldehyde (Merck Millipore, Burlington, MA, USA), pre-embedded in 1.5% agar and washed in Sorenson's phosphate buffer (pH 6.8; Morphisto, Offenbach/Main, Germany), as described previously (Budik et al., 2017). After post-fixation in 1% osmium tetroxide (Electron Microscopy Sciences, Hatfield Township, PA, USA), samples were sequentially dehydrated in ethanol series, soaked in propylene oxide and embedded in epoxy resin (Serva Electrophoresis GmbH, Heidelberg, Germany). Ultrathin sections (70 nm) were obtained with a Leica Ultramicrotome (Leica Ultracut S, Leica Microsystems, Wetzlar, Germany) and contrasted with alkaline-lead citrate (Merck Millipore) and methanolic-uranyl acetate (Sigma Aldrich, St. Louis, MO, USA). Vesicle structures were visualized on a Zeiss EM 900 transmission electron microscope (Carl Zeiss Microscopy GmbH, Jena, Germany) equipped with a digital Frame-Transfer-CCD camera (Tröndle TRS, Moorenweis, Germany).

#### 2.6. Scanning electron microscopy (SEM)

For scanning electron microscopy (SEM), sample preparation cover slips (Feix et al., 2020) were washed in 100% EtOH and coated with 0.1% poly-D-lysine (Merck Millipore, Burlington, USA) on which the isolated sexual stages were left to settle for 1 h at 36 °C in PBS. Afterwards the parasites were fixed for 3 min on the cover slip using 2.5% glutaraldehyde in PBS, and the samples were washed twice in PBS for 15 min. Post-fixation incubation was performed with 1% osmium tetroxide for 3 min. The coverslips were dehydrated in an ascending alcohol series from 30 to 100% ethanol for 3 min each. Thereafter the samples were critical point dried in a Leica CPD 300 (Leica Microsystems). The dried samples were mounted on metal stubs and gold sputtered for 80 s with a JEOL JFC-2300HR (JEOL GmbH, Freising, Germany). All SEM work was performed at the Core Facility Cell Imaging and Ultrastructure Research, University of Vienna-member of the Vienna Life-Science Instruments (VLSI), Austria. The EVs on parasite surfaces were photographed with a JEOL IT 300 scanning electron microscope (JEOL) and measured with Zeiss ZEN lite software (Carl Zeiss Microscopy GmbH).

#### 2.7. Fourier-transform infrared (FTIR) spectroscopy

The metabolic fingerprints of EVs produced by different parasite stages were analysed using Fourier Transform Infrared (FTIR) spec-

troscopy. Purified EVs from asexual, sexual, and environmental parasite stages were subjected to FTIR spectroscopy (Buchacher et al., 2023; Wong et al., 2023). Extracellular vesicle suspensions were prepared and applied to silicon optical microtiter plates (Bruker Optics GmbH, Ettlingen, Germany), then dried at 40 °C for 40 min. Spectra were recorded in transmission mode, utilizing an HTS-XT microplate adapter connected to a Tensor 27 FTIR spectrometer (Bruker Optics GmbH) with parameters set to a spectral range of 4000 to 500 cm<sup>-1</sup>, spectral resolution of 6 cm<sup>-1</sup>, and averaging 32 interferograms with background subtraction for each spectrum.

To compare FTIR spectra from EVs of different parasite stages, pre-processing involved vector normalization, baseline correction, and calculation of second derivatives across the entire spectrum using a second-order 9-point Savitzky-Golay algorithm. Spectroscopic ratios of fatty acids (3500 – 2800 cm<sup>-1</sup>), proteins (1720 – 1500 cm<sup>-1</sup>), and polysaccharides (1200 – 900 cm<sup>-1</sup>) in EVs from different origins were computed (Mihály et al., 2017; Wong et al., 2023), with minor modifications. Raw spectra were baseline corrected and smoothed using the Savitsky-Golay method (five smoothing points, third degree polynomial), followed by total integration of the specified areas. Statistical significance was determined using ANOVA ( $P < 0.05$ ). All experiments were conducted in triplicate with three biological and three technical replicates each.

#### 2.8. Proteomic analysis

S-Trap<sup>®</sup> protein digestion, as described in Mayr et al. (2024), was performed with minor modifications. In 4.5 µg of the protein lysate in RIPA buffer (Thermo Fisher), disulfide bonds were reduced with 200 mM tris(2-carboxylethyl)phosphin hydrochloride (TCEP) in 100 mM triethylammonium bicarbonate (TEAB) (1:20 v/v), alkylated with 800 mM 2-chloroacetamide (CAA) in 100 mM TEAB (1:20 v/v), SDS concentration adapted to 2% and acidified to 1% phosphoric acid. Then samples were mixed with S-Trap<sup>®</sup> buffer (90% methanol in 100 mM TEAB, 6 x the volume of the sample) and loaded onto an S-Trap<sup>®</sup> micro column (Protifi, Fairport, NY, USA) by centrifugation at 1,000 g for 1 min. Bound proteins were washed six times with 150 µl of S-Trap<sup>®</sup> buffer at 1,000 g for 1 min to remove SDS. After column drying by centrifugation at 4,000 g for 1 min, digestion was performed by adding 20 µl of Trypsin/Lys-C Mix (Promega, Madison, WI, USA; 1 µg of enzyme in 50 mM TEAB) to the S-Trap<sup>®</sup> column and incubating at 37 °C overnight without shaking. Digested peptides were eluted sequentially with 40 µl of digestion buffer (50 mM TEAB), 40 µl of 0.2% formic acid (FA), and 40 µl of 50% acetonitrile (ACN). Following drying in a vacuum concentrator, reconstituted peptides were desalted using C18 spin tips (Pierce, Thermo Fisher) as described in Mayr et al. (2024). After peptide cleanup and drying, peptides were dissolved in 45 µl of 0.1% trifluoroacetic acid (TFA) and 6 µl were injected to be analysed in technical duplicates per sample using a nano-HPLC Ultimate 3000 RSLC system coupled to a high-resolution Q-Exactive HF Orbitrap mass spectrometer (Thermo Fisher) with a 60 min gradient time HPLC method as detailed in Mayr et al. (2024).

The database search was conducted using Proteome Discoverer Software 2.4.1.15 (Thermo Fisher), with protein databases for *C. suis* (taxonomy ID 483139) and *Sus scrofa domesticus* (taxonomy ID 9825) downloaded from the UniProt homepage (<https://www.uniprot.org>) combined with the cRAP database to filter out common contaminants (<https://www.thegpm.org/crap/>). The following search parameters were set: trypsin as digestion enzyme with a maximum of two missed cleavages, fixed modification carbamidomethylation (C), variable modifications oxidation (M),

deamidation (NQ), and Gln → pyro-Glu (Q), precursor mass tolerance 10 ppm, fragment mass tolerance 0.02 Da. Proteins identified with at least two tryptic peptides and at least one unique peptide were reported and further used for intensity-based label-free quantification (LFQ). Protein abundance values were generated with Proteome Discoverer software including normalization of abundance values to total area sums. Abundance values of technical duplicates were then aggregated by the mean. In order to maintain high data quality, only proteins with zero or five abundance values per group were included in further analyses. All statistical analyses were performed in R v4.2.1 (R Core Team, 2022) with the R-script for the relative comparison of protein abundances by ANOVA including a Tukey post-hoc test as detailed in Mayr et al. (2024). Proteins with at least two identified tryptic peptides were considered to show statistically significant differences in protein abundance levels when displaying a fold change higher/lower than +/-2-fold and an adjusted *P*-value (according to Benjamini-Hochberg to compensate for multiple testing) lower than 0.05. Protein annotations for *C. suis* were obtained from <https://www.toxodb.org>, and potential homologues of *C. suis* hypothetical proteins were identified using BLAST analyses on both <https://www.toxodb.org> and <https://blast.ncbi.nlm.nih.gov/blast/Blast.cgi> with an E-value cut-off of < 0.0005. Additionally, the Kyoto Encyclopaedia of Genes and Genomes (KEGG) database (<https://www.genome.jp/kegg/kegg2.html>) was used to explore the broader biological context of the identified genes.

### 2.9. Lipidomic analysis

To analyse the lipid profile of EVs of the different parasite stages, LC-MS/MS analysis was performed on a Vanquish UHPLC system coupled to an Orbitrap Exploris 240 high-resolution mass spectrometer (Thermo Scientific, MA, USA) in negative and positive electrospray ionization (ESI) mode. Chromatographic separation was carried out on an ACQUITY Premier CSH C18 column (Waters; 2.1 mm x 100 mm, 1.7 μm) at a flow rate of 0.3 mL/min. The mobile phase consisted of water:acetonitrile (40:60, v/v; mobile phase A) and isopropanol:acetonitrile (9:1, v/v; mobile phase B), which were modified with a total buffer concentration of 10 mM ammonium acetate + 0.1% acetic acid (negative mode) and 10 mM ammonium formate + 0.1% formic acid (positive mode), respectively. The following gradient (23 min total run time including re-equilibration) was applied (min/%B): 0/15, 2.5/30, 3.2/48, 15/82, 17.5/99, 19.5/99, 20/15, 23/15. Column temperature was maintained at 65 °C, the autosampler was set to 4 °C and sample injection volume was 5 μL. Analytes were recorded via a full scan with a mass resolving power of 120,000 over a mass range from 200 – 1700 *m/z* (scan time: 100 ms, radio frequency lens: 70%). To obtain MS/MS fragment spectra, data-dependant acquisition was carried out (resolving power: 15,000; scan time: 54 ms; stepped collision energies [%]: 25/35/50; cycle time: 600 ms). Ion source parameters were set to the following values: spray voltage: 3250 V / 3000 V, sheath gas: 45 psi, auxiliary gas: 15 psi, sweep gas: 0 psi, ion transfer tube temperature: 300 °C, vaporizer temperature: 275 °C.

All experimental samples were measured in a randomized manner. Pooled quality control (QC) samples were prepared by mixing equal aliquots from each processed sample. Multiple QCs were injected at the beginning of the analysis in order to equilibrate the analytical system. A QC sample was analyzed after every fifth experimental sample to monitor instrument performance throughout the sequence. For determination of background signals and subsequent background subtraction, an additional processed blank sample was recorded. Data was processed using MS DIAL (Tsugawa

et al., 2015) and raw peak intensity data was normalized via total ion count of all detected analytes (Drotleff and Lämmerhofer, 2019). Feature identification was based on accurate mass, isotope pattern, MS/MS fragment scoring, retention time and intra-class elution pattern matching (Drotleff et al., 2020).

## 3. Results

### 3.1. Characterization of *C. suis* EVs

To gain first insights into *C. suis* EVs released by asexual, sexual and environmental stages of the parasite, nanoparticle tracking analysis was employed. The size distribution of vesicles determined that during a 2 h incubation time,  $1 \times 10^6$  intracellular (asexual and sexual) stages shed  $1 \times 10^6$  EVs (Fig. 1B), while the amount of shed EVs was five times higher in environmental stages ( $5 \times 10^6$  EVs). In a pilot experiment the optimal harvest time for EVs was determined, and EVs were released by merozoites during 1, 8, 12 and 24 h of incubation without significant differences in particle size or amount. By contrast, after 2 h of incubation the amount of shed EVs was significantly higher, and consequently, all EVs of *C. suis* were collected after this incubation time for further experiments (Fig. 1A). In general, *C. suis* EVs had a peak size ranging from 50 to 500 nm in diameter. However, most EVs of merozoites (Fig. 1C) and oocysts (Fig. 1G) were in the range of 150 nm, whereas the EV size of sexual stages was more heterogenous, as their size plateaus ranged between 150 and 200 nm (Fig. 1B and E). Interestingly, the distribution of 150 nm particles is similar among asexual and sexual stages (Fig. 1F), whereas the matched amount of EVs of doc 13 (environmental stages) is significantly higher than in the other stages (Fig. 1D and H).

To demonstrate that the isolated particles were indeed EVs and to complete their characterization, we included electron microscopy analyses. SEM revealed low amounts of EVs on all surfaces of merozoites and sexual stages incubated for 2 h at 37 °C in culture medium. The EVs of merozoites were either shed near the apical complex of the merozoite or laterally. Macrogametes showed EVs on the whole surface, whereas microgametes shed EVs primarily near the base of the flagella (Supplementary Fig. S2).

TEM analysis further confirmed that nanoparticles harvested on doc 6 and doc 10, approximately 150 nm in diameter, had intact continuous bilayer membranes (Fig. 2A and B). Merozoites showed lateral EV shedding from their cell membranes (Fig. 2C and D), while EVs transporting different cargos shed by macrogametes were found near the cell surface (Fig. 2E). In microgametes, nanoparticles were found where the flagella are attached to the body of the microgamete (Fig. 2F). In general, we were also able to show by TEM that nanoparticles differ in size and shape depending on parasite stage.

### 3.2. General cargo analysis of *C. suis* EVs

FTIR spectroscopy was used to further characterize EVs isolated from *C. suis* on doc 6, doc 10 and doc 13, and to determine their spectral metabolic fingerprint. Spectra of EVs of all parasite stages were recorded in the range of 4000 to 500  $\text{cm}^{-1}$  to determine the cargo for each parasite stage (Fig. 3A–C). Subtraction analysis of the second derivative spectrum revealed differences between the EV cargos of asexual (doc 6), sexual (doc 10) and environmental stages (doc 13). The most prominent differences between doc 13 and doc 10, as well as doc 13 and doc 6, were found in the protein region (1700–1500  $\text{cm}^{-1}$ ). The zoom-in into the region characteristic for proteins (1720–1500  $\text{cm}^{-1}$ ) and the respective second derivative subtraction showed differences between docs 6, 10 and 13, with the most prevalent differences between doc 13 and any other time

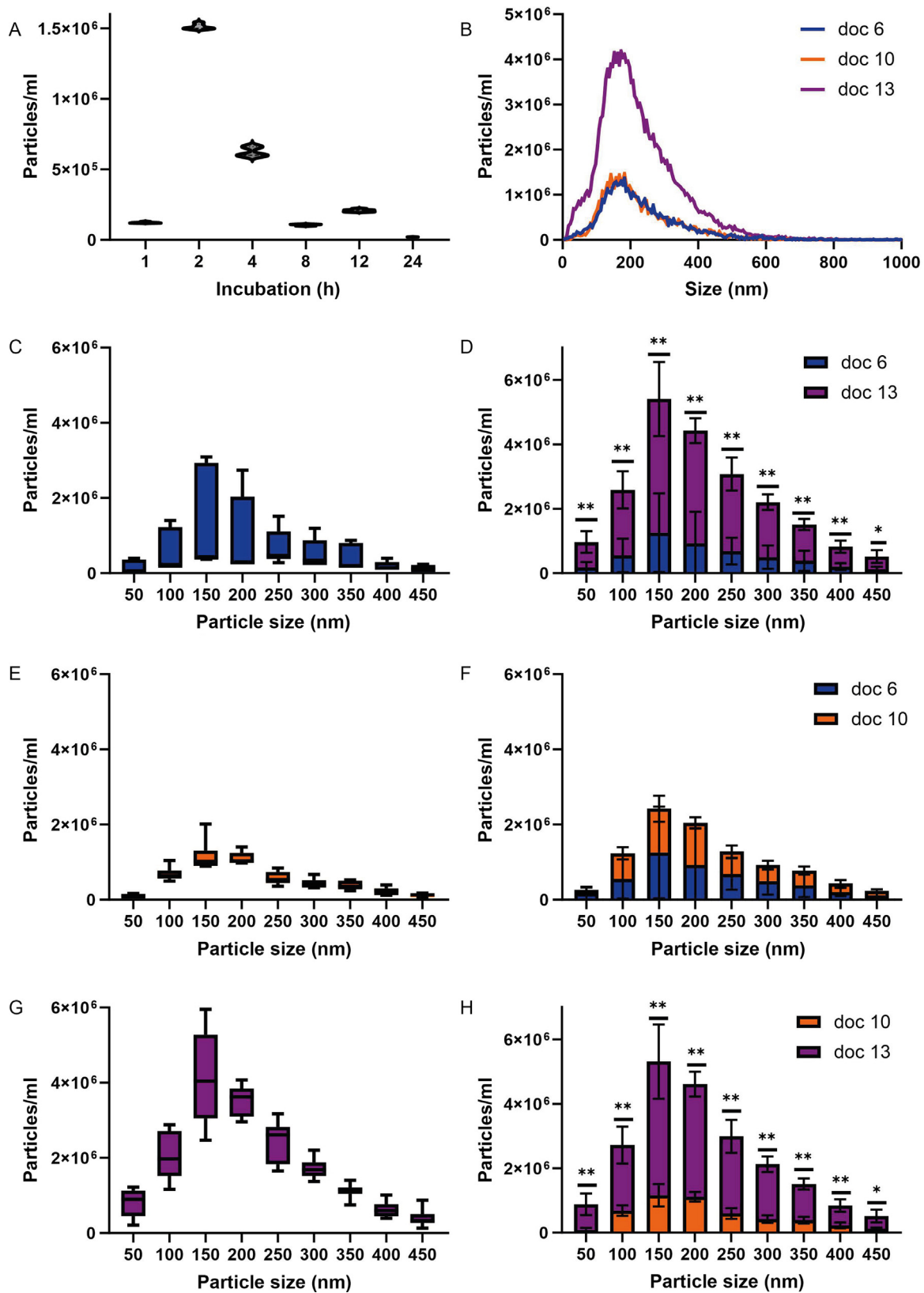


**Fig. 1.** Size distribution of purified *Cystoisospora suis* extracellular vesicles (EVs) from three biologically independent replicates (three technical measurements each) determined by Nanotracking Analysis (NTA); error bars show S.D.; significance is indicated: \* $P < 0.05$ ; \*\* $P < 0.005$ ). (A) Amount of EVs released by merozoites at 1, 2, 4, 8, 12 and 24 h of incubation. (B) Comparative size distribution of EVs shed by merozoites (day of cultivation (doc) 6, blue (black)), sexual stages (doc 10, orange (light grey)) and environmental stages (doc 13, magenta (dark grey)). (C) Size distribution of EVs of merozoites in the range of 50–450 nm. (D) Ratio of EVs from parasite stages of doc 6 and doc 13 in a particle in the size range of 50–450 nm. (E) Size distribution of EVs of sexual stages in the range of 50–450 nm. (F) Ratio of EVs from parasite stages of doc 6 and doc 10 in a particle in the size range of 50–450 nm. (G) Size distribution of EVs of oocysts in the range of 50–450 nm. (H) Ratio of EVs from parasite stages of doc 10 and doc 13 in a particle in the size range of 50–450 nm. (For interpretation of the references to colour in this figure legend, the reader is referred to the web version of this article.)

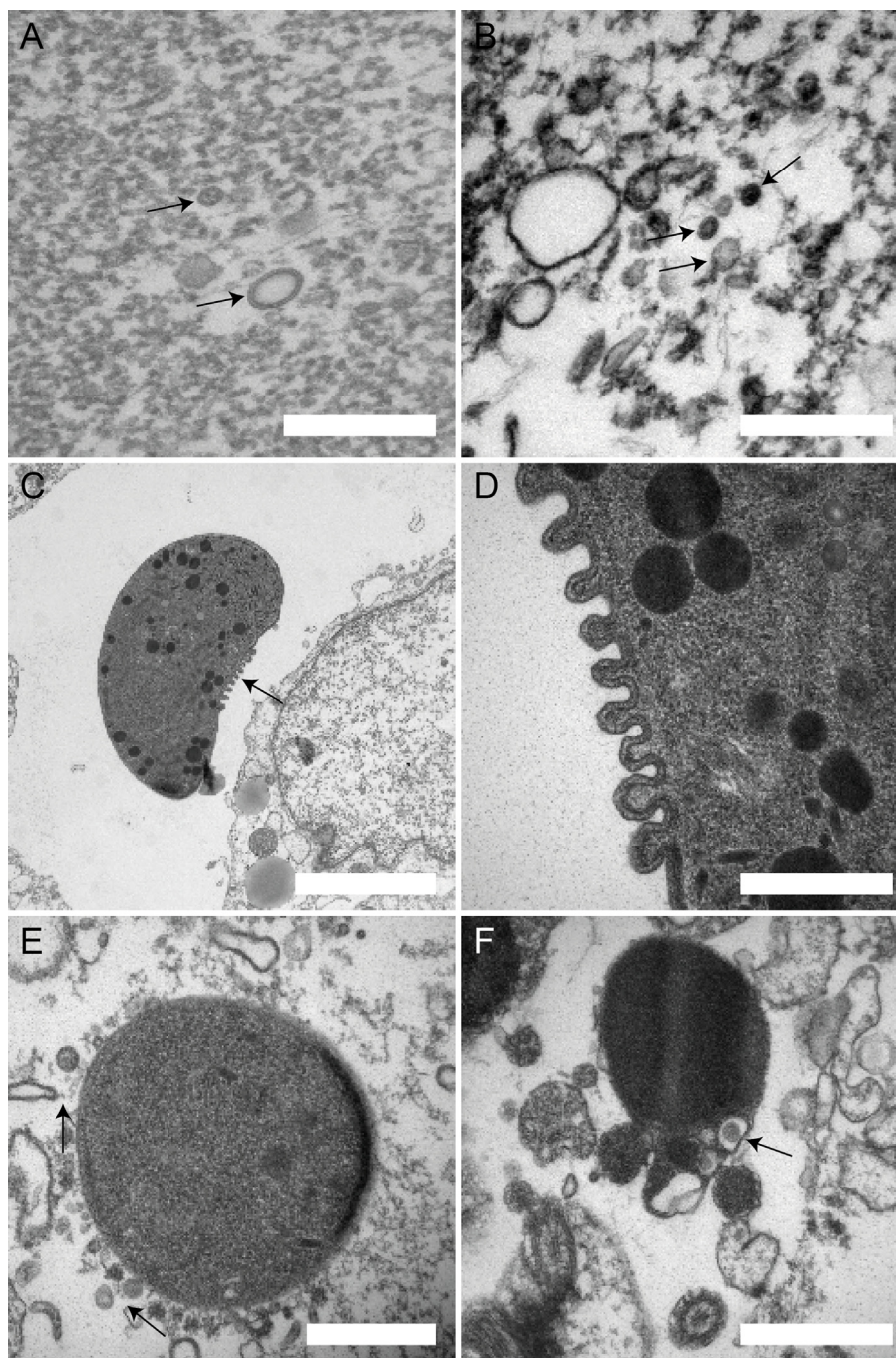


**Fig. 2.** Transmission electron microscopy of nanoparticles shed by different parasite *Cystoisospora suis* stages with arrows pointing to double membrane of extracellular vesicles (EVs). (A) EVs with a typical lipid bilayer of merozoite; scale bar = 200 nm. (B) EVs shed by sexual stages. (C and D) Merozoite (scale bar = 10  $\mu$ m) on day of cultivation (doc) 6 shedding EVs on its lateral side (scale bar = 200 nm). (E) EVs close to the surface of a macrogamete; scale bar = 20  $\mu$ m. (F) EVs located on the basal end of the flagella of a microgamete; scale bar = 2  $\mu$ m.

point (Fig. 3B and E). A tyrosine peak at 1600–1400  $\text{cm}^{-1}$  can be identified for all stages but is most apparent on doc 13 (Fig. 3C and F). These differences in the spectral regions, which are characteristic for proteins and tyrosine, were confirmed by calculating the area under the curve (AUC) of the spectral range indicative of proteins (Fig. 3G) and the tyrosine peak (Fig. 3H). Again, we could show significant differences between the AUC of oocyst EVs and EVs of merozoites or sexual stages specifically for the protein and tyrosine regions. While the AUC of the protein region stayed at a constantly lower level on doc 6 and doc 10, a significant increase in the AUC was observed on doc 13 compared with doc 6 and doc 10

(Fig. 3G), indicating changes in the protein content of the EVs. Similar differences were observed in the region indicative of the tyrosine peak, where a significant difference between doc 6 and doc 13, as well as doc 10 and doc 13, was shown (Fig. 3H).

Hierarchical cluster analysis (HCA) of the pre-processed spectra confirmed the results of FTIR subtraction spectra that EV cargo on doc 6 and doc 10, originating from previously intracellularly growing stages, is more similar to each other than to the EV cargo on doc 13, originating from sexually differentiated stages (Fig. 4A and B).

To further characterize the cargos of EVs isolated from different *C. suis* stages, we calculated the spectroscopic ratios of fatty acids

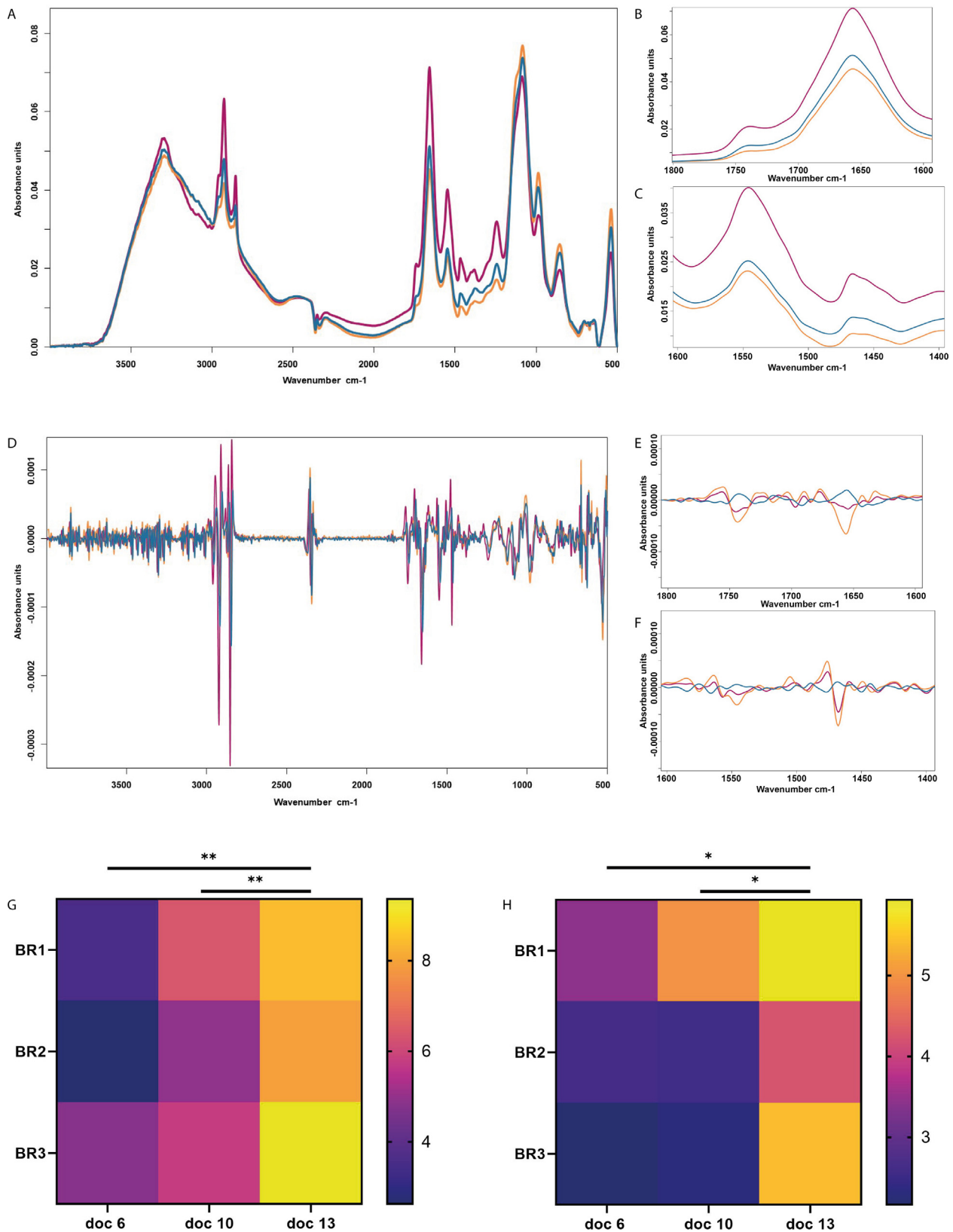


**Fig. 3.** Fourier transform infrared (FTIR) spectroscopy of extracellular Vesicle (EVs) shed from different parasite *Cystoisospora suis* stages on day of cultivation (doc) 6, 10 and 13 (three biological replicates of each day and three technical replicates by biological replicate). (A) FTIR of all stages: merozoites (blue (black)), sexual stages (orange (light grey)), oocysts (magenta (dark grey)). (B) Zoom-in into the region characteristic for proteins. (C) Zoom-in into the region characteristic for tyrosine. (D) Subtraction spectral analysis of the second derivative shows most the most prevalent differences between docs 6, 10 and 13. (E) Zoom-in of the subtraction spectral analysis characteristic for proteins. (F) Zoom-in of the subtraction spectral analysis characteristic for tyrosine. (G) Heat map of the EV protein contents on docs 6, 10 and 13 within their biological replicates (BR). (H) Heat map of the tyrosine content on docs 6, 10 and 13. Statistical significance was calculated using a two-tailed Student's *t*-test (\**P* < 0.01, \*\**P* < 0.001). (For interpretation of the references to colour in this figure legend, the reader is referred to the web version of this article.)

to proteins, fatty acids to polysaccharides and proteins to polysaccharides. The ratio of proteins to polysaccharides was stable through all parasite stages (Fig. 4D), however the ratio of fatty acids to proteins (Fig. 4B) or polysaccharides (Fig. 4C) significantly decreased. The highest ratio differences were calculated between doc 10 and doc 13, whereas a significant ratio change between doc 6 and doc 13 could only be shown for the ratio of fatty acids to proteins, although the total ratio differences were lower than differences with polysaccharides.

As significant differences within the subtraction spectra of all docs were shown for the protein, polysaccharide and tyrosine regions, we next evaluated the spectral ratio shift of these biomolecules between doc 6, doc 10 and doc 13. This showed that the amounts of protein cargo in isolated EVs on doc 6 differ most distinctly from doc 13; however, the proteins on doc 10 to doc 13 were highly similar (Fig. 4E). The spectroscopic polysaccharide cargo differed between doc 6 and doc 13, as well as doc 10 and doc 13, indicating that EV polysaccharides vary greatly during parasite development (Fig. 4F). The amount of tyrosine in EVs was highest on doc 13 in comparison to doc 6 and doc 10 (Fig. 4G).

### 3.3. The EV proteome of *C. suis* developmental stages

A total of 413 proteins were identified with at least two identified peptides, of which at least one was unique per protein, and quantified from EVs from all stages of *C. suis* (Supplementary Fig. S3, Supplementary Table S1, (PRIDE accession number **PXD057598**: <https://www.ebi.ac.uk/pride/>). Most of the identified EV proteins (73.03%,  $n = 302$ ) had significant sequence homology to known proteins of *C. suis*, and the rest were homologous within the *Sus scrofa* proteome (26.97%,  $n = 111$ ).

Among the identified molecules, ribosomal proteins, transmembrane proteins, Apicomplexa-related proteins and heat shock proteins were most prominent. To determine whether the EV samples used for proteomic analysis were uncontaminated, we analysed the occurrence of protein categories within the transmembrane proteins used as an EV hallmark. Most proteins found were transmembrane proteins associated with the plasma membrane and/or the endosome, which includes tetraspanins, transmembrane emp24 and a number of other transmembrane proteins, the functions of which are not yet known (Fig. 5A). Furthermore, a number of cytosolic proteins, i.e. heat shock proteins and actin, and trans-

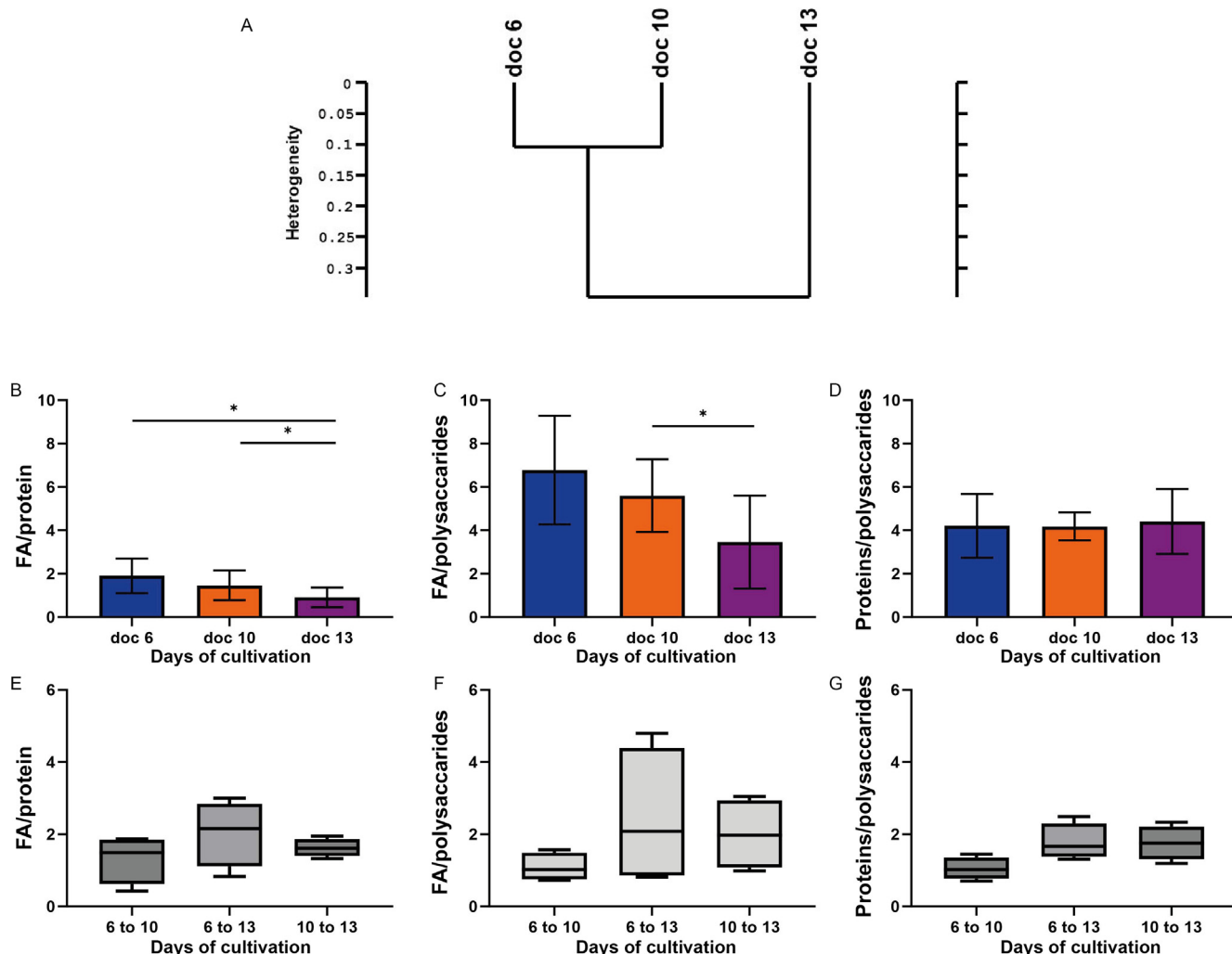


**Fig. 4.** Cargo differences of *Cystoisospora suis* extracellular vesicles (EVs) isolated on day of cultivation (doc) 6, 10 and 13; error bars show S.D.; significance is indicated: \* $P < 0.05$ . (A) Hierarchical cluster analysis shows that EV spectra on doc 6 and 10 are more similar to each other than to those harvested on doc 13; data preprocessing = vector normalization, Ward's algorithm. (B) Ratio of fatty acids (FA) to proteins. (C) Ratio of FA to polysaccharides. (D) Ratio of proteins to polysaccharides. (E) Abundance of proteins in EVs. (F) Abundance of polysaccharides. (G) Abundance of tyrosine.

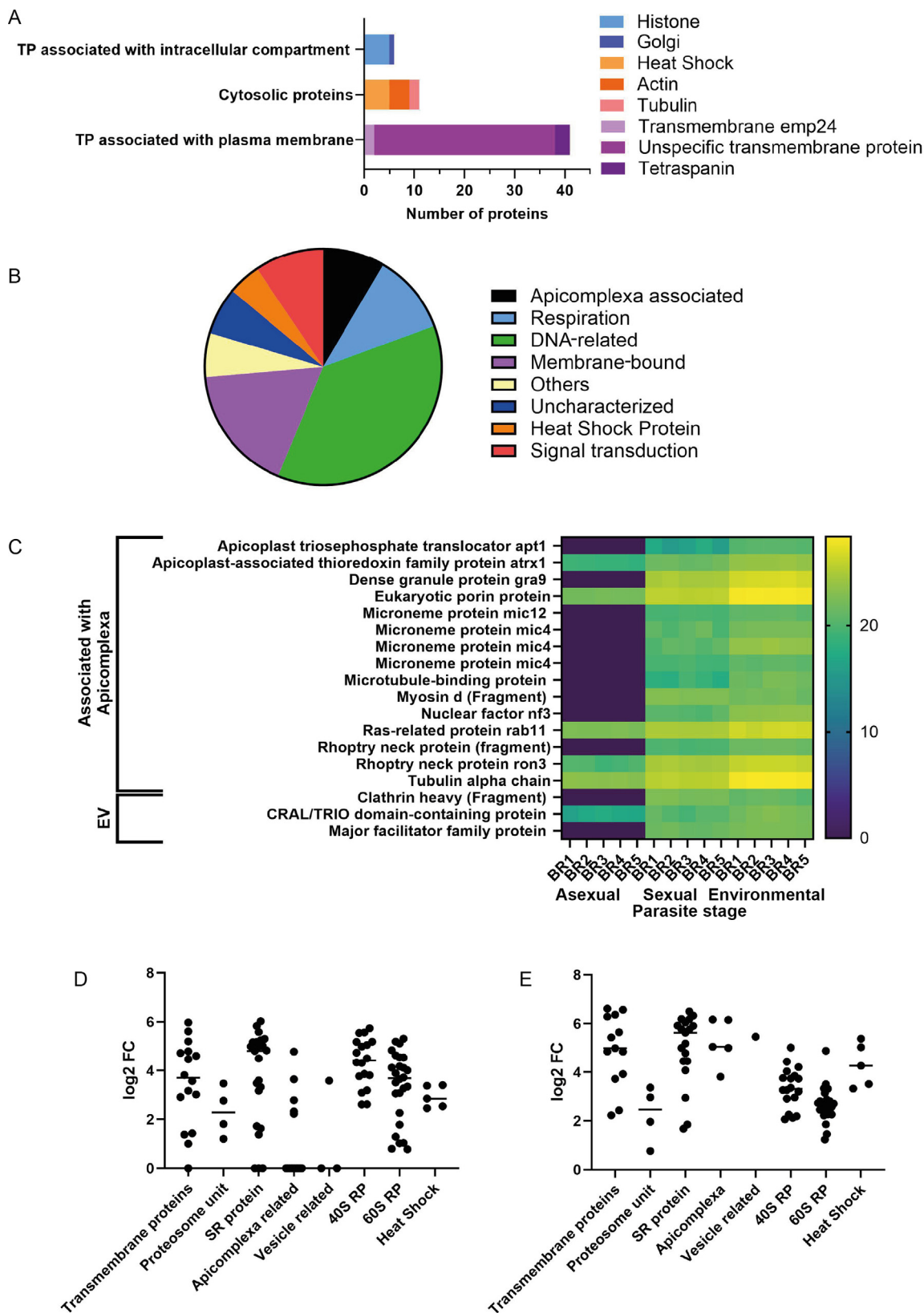


**Fig. 5.** Proteome of *Cystoisospora suis* extracellular vesicles (EVs). (A) EV hallmark proteins for the assessment of protein and isolation conditions. (B) Biological functions of up- and downregulated proteins. (C) Heat map of up- and downregulated proteins, which are specific for apicomplexan biology and for EV biogenesis in comparison with asexual, sexual and environmental parasite stages. (D) Dynamic expression pattern according to protein abundance on day of cultivation (doc) 6 to doc 10. (E) Dynamic expression pattern according to protein abundance on doc 6 to doc 13. TP, transmembrane protein; BR, biological replicates; SR, serine/arginine-rich proteins; RP, ribosomal protein; FC, fold change.

membrane, lipid-bound and soluble proteins which are more closely associated with intracellular compartments other than PM/endosomes, were found. In particular, the known markers for ectosomes and exosomes, and heat shock proteins HSP70 and HSP90, were identified in this analysis. Major components of the non-EV co-isolated structures (NVEPs) were absent from the EV proteome of *C. suis* stages.

Proteins were classified into functional categories by combining Gene Ontology (GO) predictions for *C. suis* and *Toxoplasma gondii* orthologues available in ToxoDB, together with annotations for *T. gondii* from the KEGG pathway database, BLAST homology searches, and recent literature. Only 13.3% of proteins could not be classified into any of the various categories. We were able to identify 8.5% as Apicomplexa-specific proteins, reflecting a diverse range of biological activities of these proteins and underscoring the complex interplay of various cellular functions (Fig. 5B).

The abundance of proteins associated with apicomplexans showed clear shifts between asexual, sexual, and environmental parasite stages. The proteins were categorized into those closely associated with proteins important for the apicomplexan life cycle and those which are involved in EV biogenesis. Notably, the EV-associated proteins such as Clathrin show relatively higher abundance compared with most other proteins, suggesting that the EV-associated proteins in general are more prominent compared with other proteins in the dataset. Among the proteins associated with apicomplexans, microneme protein mic4 and rhoptry neck protein ron3 exhibited notable increases in the sexual and environmental stages. Apicoplast-associated thioredoxin family protein atrx1 and eukaryotic porin protein were consistently present across all stages but at moderate to lower levels. The overall pattern suggests differential regulation of these key proteins depending on the life cycle stage of the parasite (Fig. 5C).

The dynamic expression pattern based on protein abundance (Fig. 5D and E) highlights significant differences in protein expression across developmental stages. Notably, the abundance of transmembrane proteins, apicomplexan-specific proteins, and vesicle-related proteins varied between asexual and sexual stages, as well as between asexual and environmental stages. Specifically, the abundance of these proteins was lowest on doc 6 and consistently increased until doc 13.

### 3.4. The EV lipidome of *C. suis* developmental stages

The EV lipid composition obtained from all parasite stages showed that 441 lipid species (Supplementary Table S2) representing five superclasses (i.e. fatty acyls, FA; glycerolipids, GL; glycerophospholipids, GP; sphingolipids, SP; and sterol lipids, SL) were identified and quantified (Fig. 6A). Almost 78% of lipid species identified in EVs belonged to the categories GP and SP, while only limited lipid species represented categories GL, SL and FA. Unlike lipid profiles of other apicomplexan species, we were able to observe that within the specific EV-only lysate, GP dominate the identified lipid species, whereas only three different GL species were detected (Fig. 6B). The analysis of fatty acyls, which were expected to be highly specific as seen in the FTIR-spectra for all parasite stages (Fig. 3A), revealed distinct variations in their composition. Unsaturated fatty acids were the most prevalent class, followed by saturated fatty acids. Fatty acids in general account for 44 identified species, including a smaller subset of oxidized fatty acids. Overall, unsaturated and saturated fatty acids predominated, while oxidized fatty acids represented only a minor component of the overall fatty acid profile (Fig. 6C). Specifically, within the GP class (Fig. 6D), glycerophosphocholines were the most prevalent, followed by glycerophosphoethanolamines, glycerophosphoinositols, glycerophosphoserines, glycerophosphoglycerols, and cardiolipins. The analysis of SP revealed a diverse

distribution among different classes. Ceramides were the most abundant sphingolipid class identified, followed by glycosphingolipids and phosphosphingolipids. Neutral glycosphingolipids were less prevalent, and sphingoid bases were the least common (Fig. 6E). This distribution highlights the significant presence of complex sphingolipid species, such as ceramides and glycosphingolipids, within the samples.

Several lipid species, particularly sterolipids and glycerolipids, show significant changes in abundance during parasite development, when comparing their expression on doc 6 versus doc 10 (Fig. 6F) and doc 6 versus doc 13 (Fig. 6G). Between doc 6 and doc 10, phosphatidylcholines and lysophosphatidylcholines exhibit significant upregulation. Additionally, certain sphingolipids such as ceramides and glycosphingolipids also show substantial upregulation, showing an increase in specific sterolipids and sphingolipids from asexual to sexual stages (Fig. 6F). Similarly, most lipids have been downregulated from doc 6 samples to doc 13 samples and only lipids of three superclasses (GL, SL, SP) have been found. Glycerolipids have mainly been downregulated from asexual to environmental stages, whereas sphingolipids were mainly upregulated. Specifically, SP such as ceramides and glycosphingolipids also show substantial upregulation from asexual to environmental parasite stages.

## 4. Discussion

*Cystoisospora suis* is a coccidian species that can be cultivated in vitro throughout the whole life cycle and provides host tissue-free material for analyses, which is a significant advantage compared with *T. gondii* when it comes to studies on sexual stages. All developmental stages of *C. suis* occur in vitro, extracellularly at specific time slots, which is the prerequisite for host cell-free isolation and incubation of the parasites (Feix et al., 2020, 2021). We successfully developed an EV isolation protocol for all parasite stages of *C. suis* that included harvesting and cleaning of parasite stages, incubation in EV-free medium, filtering of EVs, ultracentrifugation and characterization by NTA, and FTIR, in addition to electron microscopy for morphological studies on the site of shedding.

Currently, no specific guidelines for isolating EVs from apicomplexan parasites such as *C. suis* exist, unlike those for eukaryotic EVs in MISEV2018 (Théry et al., 2018) or for helminths (White et al., 2023). Therefore we used differential centrifugation to isolate *C. suis* EVs. Parasitic cells and debris are removed, followed by EV concentration and ultracentrifugation to pellet EVs (Zoia et al., 2022). While density gradients and size exclusion chromatography are generally considered optimal for EV isolation, salt conglomerations from density gradients affected fresh EV samples from material in this study, causing a size shift in NTA analysis and skewed proteomics results. Therefore, we opted for differential centrifugation and enrichment as previously described (Théry et al., 2018; Zoia et al., 2022; Omari et al., 2023; Welsh et al., 2024).

*Cystoisospora suis* EVs ranged from 50 to 500 nm in size, including both the small exosomes and the ectosomes which are more heterogeneous in shape and in diameter (Hugel et al., 2005). Our results strongly support the hypothesis that all stages of *C. suis* actively produce and secrete EVs of variable sizes into the extracellular milieu during the parasite's development in vitro (and presumably also in vivo). This heterogeneity was also shown by morphological analysis (NTA) and demonstrated by TEM. While SEM indicated that EVs of merozoites are shed at the apical end, near the apical complex of the cells (Supplementary Fig. S2), TEM analysis showed that merozoites incubated for 2 h shed their EVs laterally on the convex side of their surface. As the differences in EV sizes, cargos and functions are vast, we assume that the two

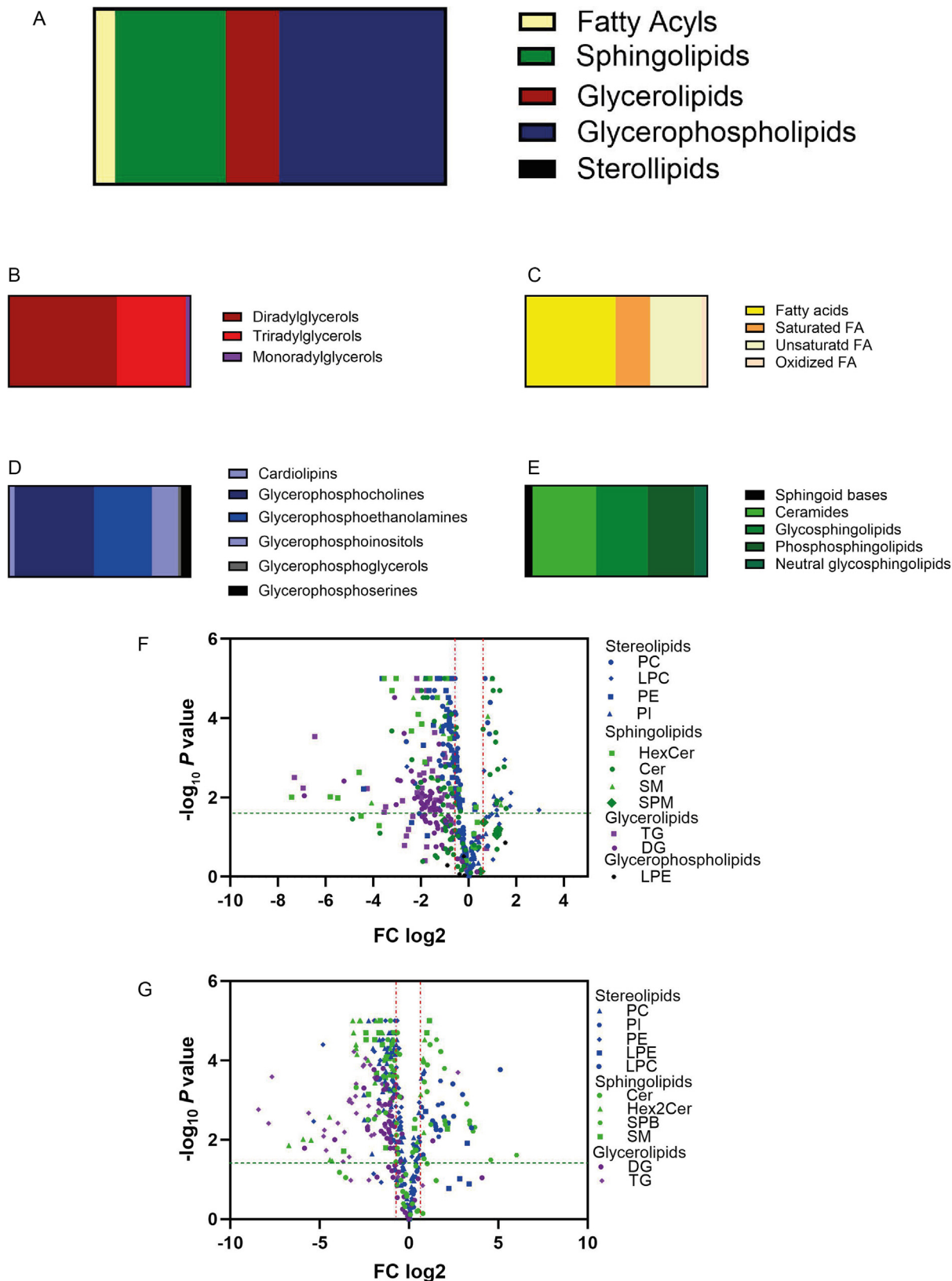


**Fig. 6.** Lipidome of *Cystoisospora suis* extracellular vesicles (EVs). (A) Lipid super classes found in EVs of all parasite stages. (B) Glycolipids (GL) found in EVs of all parasite stages. (C) Fatty acyls (FA) found in EVs of all parasite stages. (D) Glycerophospholipids (GP) found in EVs of all parasite stages. (E) Spingolipids (SP) found in EVs of all parasite stages. (F) Volcano plot of up- and downregulation of all lipid super classes between day of cultivation (doc) 6 and doc 10. (G) Volcano plot of up- and downregulation of all lipid super classes between doc 6 and doc 13. Lipids with significant changes in expression are those further from the centre on the X-axis and higher on the Y-axis, indicating greater fold changes and higher statistical significance. The red dashed vertical lines at log<sub>2</sub> fold changes (FC) of ± 1 indicate thresholds for significant upregulation or downregulation. nGP = 354, nSP = 240, nGL = 116, nSL = 3, nFA = 44. SL, stereolipids; PC, phosphatidylcholine; LPC, lysophosphatidylcholine; PE, phosphatidylethanolamine; PI, phosphatidylinositol; LPE, lysophosphatidylethanolamine; HexCer, hexosylceramide; Cer, ceramide; SM, sphingomyelin; SPM, sphingosine-1-phosphate; SPB, sphingosine-phosphate binding protein; TG, triacylglycerol; DG, diacylglycerol; LPE, lysophosphatidylethanolamine. (For interpretation of the references to colour in this figure legend, the reader is referred to the web version of this article.)

methods depicted two different types of EVs shed from different locations of the parasite cell. Most EVs shed by merozoites and sexual stages were 150 nm in size, which is typical for ectosomes used for intercellular communication (Raposo and Stoorvogel, 2013). However, the number of particles shed on doc 10, on which the sexual stages, micro- and macrogametes occur, was significantly lower than on the other days. As with all Coccidia, the life cycle of *C. suis* is characterized by a switch from asexual merogony to sexual development of gametes (Feix et al., 2020; Cruz-Bustos et al., 2021). The gross number of sexual stages is significantly reduced compared with stages during asexual development but still sufficient for micro- and macrogametes to fuse to a zygote and complete their life cycle with the formation of an oocyst (Feix et al., 2020, 2021). Therefore, the amount of EVs shed on doc 10 correlates with the lower amount of sexual parasite stages, and depicts the developmental bottleneck of Coccidia during sexual development (Smith et al., 2014).

Furthermore, correlations between different developmental stages and the cargos transported by their EVs to other parasite and host cells were found. The spectral fingerprint of *C. suis* EVs showed a high content of fatty acids, proteins and polysaccharides in all parasite stages. Spectral subtraction analysis of the second derivative spectra revealed differences between the EV cargos of asexual (doc 6), sexual (doc 10) and environmental stages (doc 13). The most prominent differences between oocysts and sexual stages, as well as oocysts and merozoites, were found in the protein region. Functional annotation revealed that the most prevalent functional categories were proteins related to DNA processing and respiration. Furthermore, FTIR spectroscopy identified a prominent absorption peak near  $1080\text{ cm}^{-1}$ , attributed to phosphate groups present in nucleic acids. This absorption is specifically linked to the symmetric stretching of  $\text{PO}_2^-$  groups within the phosphodiester backbone, a critical structural element in DNA and RNA (Balduzzi et al., 2024). As anticipated, proteins which are predicted to have various functions with roles in parasite biology, such as membrane components and apicomplexan-associated proteins, were shown by mass spectrometry. Two protein families, tyrosine-rich and cysteine-rich proteins, detected by FTIR (Davis and Mauer, 2010; Yang and Arrizabalaga, 2017), are highly important for coccidians as they participate in oocyst wall formation (Belli et al., 2003). Although tyrosin-rich proteins have already been demonstrated in *C. suis* sexual stages and oocysts (Feix et al. 2020, 2021; Cruz-Bustos et al., 2023), their transfer through EVs could not be shown yet. Zhao et al. (2018) suggested that tyrosine phosphorylation might have a more general role in regulating extracellular vesicle shedding in eukaryotic tumour cells. For *C. suis* this could also indicate that the increased tyrosine in EVs might not only be due to an increased demand for tyrosine in oocyst formation, but also due to increased EV shedding.

A more detailed proteomic study allowed not only identification of specific proteins such as dense granule proteins and microneme proteins which are specific for apicomplexans (Butler et al. 2014), or proteins which are key for EV shedding (Leung et al., 2008), but also showed the cleanness of the preparation by ultracentrifugation. We utilized the MISEV guidelines to characterize the proteome of EVs from *C. suis*, focusing on protein content-based EV characterization. Specifically, we analysed the occurrence of protein categories within the transmembrane proteins used as an EV hallmark from categories 1, 2 and 4 (Thery et al., 2018; Welsh et al., 2024) to confirm the nature of the EV and to assess the purity of the EV preparation and enrichment with different centrifugation steps. While the guidelines provide examples of proteins commonly found in mammalian cell-derived EVs, we also considered other proteins fitting these categories, particularly those relevant to EVs from non-mammalian eukaryotic sources such as invertebrate parasites. A comparison with the proteomes

of EVs from *T. gondii* revealed proteins in the EV lysate with similar or identical biological functions to those in *C. suis*, with metabolism-related proteins being abundant in both (Wowk et al., 2017). As anticipated, HSP70 and HSP90, known markers for ectosomes and exosomes, similar to *T. gondii*, were identified in *C. suis*. The normalized data demonstrate that HSP expression remains stable across all stages of *C. suis*, without observed changes during the environmental stages. This stability suggests that HSPs could serve as reliable EV markers. However, in the present study, no specific enrichment of EV fractions, including HSP, was conducted, as we aimed to identify general EV protein profiles rather than isolating or enhancing specific protein subsets. Although we expected to detect dense granule (GRA) proteins, as they are prominent in *T. gondii* EVs (Ramirez-Flores et al., 2019), these were not found in the *C. suis* samples. The high number of microneme (MIC) proteins in our sample might be attributed to their continuous secretion during parasite motility, a phenomenon also observed in *T. gondii*, where the highest concentration of MIC proteins was found in a pure supernatant fraction (Ramirez-Flores et al., 2019).

No specific antibodies for *C. suis* could be validated for Western blotting or other immunodetection techniques. While established EV markers such as CD63, TSG101, Alix, and HSP70 are frequently used in mammalian systems, they are often absent or poorly conserved in apicomplexan parasites (Szemppruch et al., 2016; Yong et al., 2021). Instead, HSPs such as HSP70 and HSP90, which are more universally conserved across diverse organisms, have been employed to identify EVs of apicomplexans. However, this strategy did not yield effective detection results in our studies of *C. suis*. In some cases, parasite-specific proteins have proven valuable for EV identification in related apicomplexans. For example, PfEMP1 and RESA have been effectively used in *Plasmodium falciparum* research (Mantel and Marti, 2014), and SAG1 together with GRA proteins are common markers in *T. gondii* (Silva et al., 2019), but these parasite-specific proteins were scarce in our *C. suis* EV protein extracts, rendering them unsuitable for western blot (WB) applications. However, for future applications, tailored antibody application should improve EV-based studies in non-model apicomplexan parasites such as *C. suis*.

The polysaccharide populations differed markedly between sexual stages and oocysts of *C. suis*. Polysaccharide synthesis by sexual stages is part of the preparation for cyst formation in cyst-forming coccidians (Scholtyssek and Hammond, 1970). The presence of starch metabolism (polysaccharide storage) and trehalose synthesis pathways in coccidians and *Cryptosporidium* is indicative of this adaptation (Shanmugasundram et al., 2013) and explains why polysaccharides were prevalent in EVs through all investigated parasite stages. The constant shedding of polysaccharides hints at a possible function of those EVs in inter-cellular communication. However, although parasite-derived polysaccharides have been shown to drive the conversion of tachyzoites (replicating stages) to bradyzoites (resting stages) in *Toxoplasma* (Skariah et al., 2010), the function of EVs in conveying such molecules to other cells still remains to be elucidated.

Although the lipid bilayer of EVs is a characteristic attribute, its structure and composition is still poorly understood (Skotland et al., 2020). The abundance of GP and SP in the EVs of *C. suis* can be attributed to several key factors related to the biological roles and biogenesis of these vesicles. Glycerophospholipids such as phosphatidylcholines and phosphatidylethanolamines are fundamental components of cellular membranes, including those of EVs, providing structural integrity and fluidity essential for vesicle formation and function (Llorente et al., 2013; Skotland et al., 2020). Sphingolipids, including ceramides and glycosphingolipids, play crucial roles in cell signalling, membrane organization, and the formation of lipid rafts, which are specialized microdomains

critical for EV budding and cargo sorting (van Meer et al., 2008; Hallal et al., 2022). Additionally, SP may be involved in host-pathogen interactions, facilitating the delivery of parasitic molecules to host cells, modulating immune responses, and enhancing parasite survival and virulence (Wang et al., 2021; Matos et al., 2023). In apicomplexan parasites such as *T. gondii* and *Eimeria falciformis*, lipid composition in EVs supports mechanisms of immune modulation and nutrient acquisition, enabling the parasite to adapt within host environments. For example, *T. gondii* EVs hijack host lipid pathways, redirecting host lipid resources to enhance parasite survival under nutrient-limited conditions. Meanwhile, *E. falciformis* EVs modulate host inflammatory responses, promoting a permissive environment for infection (Olajide et al., 2023). Ceramides play crucial roles in the biology of apicomplexan parasites, significantly contributing to their survival, pathogenicity, and interaction with host organisms. Acting as bioactive lipid mediators, ceramides are involved in various cellular signalling pathways that regulate processes such as cell differentiation and proliferation, which are vital for parasite development and lifecycle progression (Nyonda et al., 2022; Koutsogiannis et al., 2023). This regulatory function likely explains the upregulation of ceramides observed in the sexual and environmental stages of *C. suis*. This modulation facilitates the evasion of host immune defences, thereby enhancing parasite survival within host tissues (Nyonda et al., 2022).

Since fatty acids are prominent in EVs from all parasite stages, both during FTIR and lipidomic analysis with mass spectroscopy, their importance cannot be ignored. The assumption that apicomplexans lack the ability to synthesize fatty acids and are dependent on their hosts was recently revised, and lipids in general have emerged as important pathogenesis factors in a variety of infectious diseases (Mazumdar et al., 2007; Welti et al., 2007). Exosomes and ectosomes are capable of directly transporting lipids, amides, fatty acids, and eicosanoids, from producing to recipient cells, which can induce changes in immune response and cellular metabolism (Wang et al., 2020). It is therefore conceivable that the asexual (multiplying) stages of apicomplexan parasites employ lipid EVs for intercellular communication to accelerate their proliferation, and therefore drive the severity and/or chronicity of parasite infection.

In summary, despite increasing interest in the composition and function of EVs in the maintenance of physiological processes and in diseases, especially cancer, they have so far been somewhat neglected in the field of parasitic protozoa. Based on previous basic studies in apicomplexans and advanced protocols for standardised EV isolation, we here developed a protocol for EV isolation and analysis for *C. suis* and, on a wider scale, for apicomplexan parasites. Furthermore, we analysed different stages, from asexual multiplication to sexual differentiation and the development of transmissible stages, in a so far unique culture model for coccidians, to compare the morphology and composition of EVs during the in vitro development of *C. suis* as a member of the cyst-forming coccidians. Overall, our study will enable accelerated research on, and improved detailed analyses of, coccidian (and apicomplexan) EVs, which will be of utmost importance in elucidating the role of EVs in parasite biology (especially sexual development, gamete fusion and zygote formation) and parasite-host interactions.

Deciphering the contributions of EVs to parasite infection and development will further aid the development of novel strategies to combat parasitic infections. This is especially important since resistance against commonly used antiparasitic drugs against apicomplexans are on the rise, and there is an increased need for novel treatment methods. The role of EVs as transport vesicles for new treatments has only been utilised in the past years, using a “trojan horse strategy” for drug delivery and targeted applica-

tions of EVs (Pendiuk Goncalves et al., 2023). While apicomplexan EVs are not yet routinely used in infectious disease diagnostics or therapeutics, promising strategies are emerging. To advance EV applications in clinical settings, cost-effective, scalable production methods are essential, enabling high-throughput biomarker research and EV-based therapies. However, in other apicomplexans some promising proteins were already identified. *Plasmodium falciparum* EVs contain invasion-associated proteins and are internalized by immune cells, prompting innate immune responses. Similarly, EVs from *T. gondii* (Li et al., 2018), *Giardia duodenalis* (Faria et al., 2023), and *Trypanosoma cruzi* (Bayer-Santos et al., 2014) activate macrophage inflammatory responses through enhanced cytokine production and TLR2 and NLRP3 pathways, while *T. cruzi* EVs also inhibit C3 of the complement pathway, aiding immune evasion. Notably, *T. gondii* EVs increase IFN- $\gamma$  and reduce IL-10, enhancing protection as shown by antibody production and improved survival in animal models (Li et al., 2018). These findings indicate that protozoan parasite EVs are immunostimulatory and strategically balanced, providing a complex mechanism for immune modulation and potential future use in diagnostics, therapeutics, and vaccines against protozoan infections.

The identification of critical attributes, sufficient to achieve long-distance targeting of protozoan parasites, is crucial to mitigate risks associated with the high complexity of this system. Hence research on apicomplexan EVs is still in the early stages, but will accelerate research and drug development in the future.

#### CRedit authorship contribution statement

**Anna Sophia Feix:** Writing – original draft, Formal analysis, Data curation, Conceptualization. **Astrid Laimer-Digruber:** Writing – review & editing, Methodology. **Teresa Cruz-Bustos:** Methodology. **Gerhard Steiner:** Resources. **Bärbel Ruttkowski:** Methodology. **Monika Ehling-Schulz:** Resources. **Anja Joachim:** Writing – review & editing, Funding acquisition.

#### Acknowledgments

We would like to thank Sonja Rohrer from the Institute of Parasitology, Vetmeduni Vienna, Austria, for taking care of the piglets used for oocyst collection for this study, as well as VetImaging of the University of Veterinary Medicine Vienna, Austria, especially Dr Ursula Reichart for her expertise in all performed immunofluorescence work, Waltraud Tschulenk (Institute of Morphology, Vetmeduni Vienna) for her expertise in TEM and Daniela Gruber of the Core Facility Cell Imaging and Ultrastructure Research, University of Vienna (Austria) a member of the Vienna Life-Science Instruments (VLSI) for her expertise in all performed scanning electron microscopy work. This research was supported using resources of the VetCore Facility (Imaging/Mass Spectrometry/Genomics) of the University of Veterinary Medicine Vienna. All methods were performed in accordance with the guidelines and regulations approved by the University of Veterinary Medicine Vienna and the national authority (Austrian Federal Ministry of Science, Health and Economy). The study is reported in accordance with ARRIVE guidelines. All procedures in this study involving experimental animals were performed under the direct supervision of a veterinary specialist, and were approved by the institutional ethics and animal welfare committee (Ethik- und Tierschutzkommission) of the University of Veterinary Medicine Vienna and the national authorities according to §§26ff. of the Animal Experiments Act, Tierversuchsgesetz 2021 – TVG 2012 (Austrian Federal Ministry of Science, Health and Economy) under license number 2021-0.030.760. All efforts were made to minimize the number of ani-

mals used for *C. suis* oocyst generation. This research was funded in whole by the Austrian Science Fund (FWF; grant no.: P 33123-B).

## Appendix A. Supplementary material

Supplementary data to this article can be found online at <https://doi.org/10.1016/j.ijpara.2025.01.001>.

## References

- Bachurski, D., Schuldner, M., Nguyen, P.H., Malz, A., Reiners, K.S., Grenzi, P.C., Babatz, F., Schauss, A.C., Hansen, H.P., Hallek, M., Pogge von Strandmann, E., 2019. Extracellular vesicle measurements with nanoparticle tracking analysis - An accuracy and repeatability comparison between NanoSight NS300 and ZetaView. *J Extracell Vesicles* 8 (1), 1596016. <https://doi.org/10.1080/20013078.2019.1596016>.
- Barta, J.R., Schrenzel, M.D., Carreno, R., Rideout, B.A., 2005. The genus *Atoxoplasma* (Garnham 1950) as a junior objective synonym of the genus *Isoospora* (Schneider 1881) species infecting birds and resurrection of *Cystoisospora* (Frenkel 1977) as the correct genus for *Isoospora* species infecting mammals. *J. Parasitol.* 91, 726–727. <https://doi.org/10.1645/ge-3341.1>.
- Bayer-Santos, E., Lima, F.M., Ruiz, J.C., Almeida, I.C., Da Silveira, J.F., 2014. Characterization of the small RNA content of *Trypanosoma cruzi* extracellular vesicles. *Mol. Biochem. Parasitol.* 193 (2), 71–74. <https://doi.org/10.1016/j.molbiopara.2014.02.004>.
- Belli, S.I., Wallach, M.G., Luxford, C., Davies, M.J., Smith, N.C., 2003. Roles of tyrosine-rich precursor glycoproteins and dityrosine- and 3,4-dihydroxyphenylalanine-mediated protein cross-linking in development of the oocyst wall in the coccidian parasite *Eimeria maxima*. *Eukaryot. Cell* 2 (3), 456–464. <https://doi.org/10.1128/ec.2.3.456-464.2003>.
- Buchacher, T., Digruber, A., Kanzler, M., Del Favero, G., Ehling-Schulz, M., 2023. *Bacillus cereus* extracellular vesicles act as shuttles for biologically active multicomponent enterotoxins. *Cell Commun. Signal* 21, 112. <https://doi.org/10.1186/s12964-023-01132-1>.
- Budik, S., Tschulen, W., Kummer, S., Walter, I., Aurich, C., 2017. Evaluation of SmartFlare probe applicability for verification of RNAs in early equine conceptuses, equine dermal fibroblast cells and trophoblastic vesicles. *Reprod. Fertil. Dev.* 29 (11), 2157–2167. <https://doi.org/10.1071/RD16362>.
- Butler, C.L., Lucas, O., Wuchty, S., Xue, B., Uversky, V.N., White, M., 2014. Identifying novel cell cycle proteins in Apicomplexa parasites through co-expression decision analysis. *PLoS One* 9 (5), e97625. <https://doi.org/10.1371/journal.pone.0097625>.
- Coakley, G., Buck, A.H., Maizels, R.M., 2016. Host parasite communications – Messages from helminths for the immune system: Parasite communication and cell-cell interactions. *Mol. Biochem. Parasitol.* 208, 33–40. <https://doi.org/10.1016/j.molbiopara.2016.06.003>.
- Coakley, G., Mc Caskill, J.L., Borger, J.G., Simbari, F., Robertson, E., Millar, M., Harcus, Y., McSorley, J., Maizels, R.M., Buck, A., 2017. Extracellular vesicles from a helminth parasite suppress macrophage activation and constitute an effective vaccine for protective immunity. *Cell Rep.* 19, 1545–1557. <https://doi.org/10.1016/j.celrep.2017.05.001>.
- Cruz-Bustos, T., Feix, A.S., Ruttkowski, B., Joachim, A., 2021. Sexual development in non-human parasitic Apicomplexa: Just biology or targets for control? *Animals* 11, 1–18. <https://doi.org/10.3390/ani11102891>.
- Cruz-Bustos, T., Dolezal, M., Feix, A.S., Ruttkowski, B., Hummel, K., Razzazi-Fazeli, E., Joachim, A., 2023. Unravelling the sexual developmental biology of *Cystoisospora suis*, a model for comparative coccidian parasite studies. *Front. Cell. Infect. Microbiol.* 13, 1271731. <https://doi.org/10.3389/fcimb.2023.1271731>.
- Davis, R., Mauer, L.J., 2010. Fourier transform infrared FT-IR spectroscopy: A rapid tool for detection and analysis of foodborne pathogenic bacteria. *Curr Res Technol Educ Top Appl Microbiol Microb Biotechnol* 2, 1582–1594. <https://doi.org/10.1021/jf049354q>.
- Drotleff, B., Lämmerhofer, M., 2019. Guidelines for selection of internal standard-based normalization strategies in untargeted lipidomic profiling by LC-HR-MS/MS. *Anal. Chem.* 91 (15), 9836–9843. <https://doi.org/10.1021/acs.analchem.9b01505>.
- Drotleff, B., Roth, S.R., Henkel, K., Calderón, C., Schlotterbeck, J., Neukamm, M.A., Lämmerhofer, M., 2020. Lipidomic profiling of non-mineralized dental plaque and biofilm by untargeted UHPLC-QTOF-MS/MS and SWATH acquisition. *Anal. Bioanal. Chem.* 412 (10), 2303–2314. <https://doi.org/10.1007/s00216-019-02364-2>.
- Druey, C., Maizels, R.M., 2021. Helminth extracellular vesicles: Interactions with the host immune system. *Mol. Immunol.* 137, 124–133. <https://doi.org/10.1016/j.molimm.2021.06.017>.
- Faria, C.P., Ferreira, B., Lourenço, Á., Guerra, I., Melo, T., Domingues, P., Domingues, M.D.R.M., Cruz, M.T., Sousa, M.D.C., 2023. Lipidome of extracellular vesicles from *Giardia lamblia*. *PLoS One* 18 (9), e0291292. <https://doi.org/10.1371/journal.pone.0291292>.
- Feix, A.S., Cruz-Bustos, T., Ruttkowski, B., Joachim, A., 2020. Characterization of *Cystoisospora suis* sexual stages *in vitro*. *Parasit. Vectors* 13, 143. <https://doi.org/10.1186/s13071-020-04014-4>.
- Feix, A.S., Cruz-Bustos, T., Ruttkowski, B., Mötz, M., Rümnapf, T., Joachim, A., 2021. Progression of asexual to sexual stages of *Cystoisospora suis* in a host cell-free environment as a model for Coccidia. *Parasitology* 148, 1475–1481. <https://doi.org/10.1017/S0031182021001074>.
- Feix, A.S., Cruz-Bustos, T., Ruttkowski, B., Joachim, A., 2023. *In vitro* cultivation methods for coccidian parasite research. *Int. J. Parasitol.* 53 (9), 477–489. <https://doi.org/10.1016/j.ijpara.2022.10.002>.
- Fridman, E.S., Ginini, L., Gil, Z., 2022. The role of extracellular vesicles in metabolic reprogramming of the tumor microenvironment. *Cells* 11 (9), 1433. <https://doi.org/10.3390/cells11091433>.
- Hallal, S., Túzesi, Á., Grau, G.E., Buckland, M.E., Alexander, K.L., 2022. Understanding the extracellular vesicle surface for clinical molecular biology. *J Extracell Vesicles* 11 (10), e12260. <https://doi.org/10.1002/jev2.12260>.
- Hugel, B., Martínez, M.C., Kunzelmann, C., Freyssinet, J.M., 2005. Membrane microparticles: two sides of the coin. *Physiology* 20, 22–27. <https://doi.org/10.1152/physiol.00029>.
- Isaac, R., Castellani, F., Reis, G., Ying, W., Olefsky, J.M., 2021. Exosomes as mediators of intercellular crosstalk in metabolism. *Cell Metab.* 33, 1744–1762. <https://doi.org/10.1016/j.cmet.2021.08.006>.
- Joachim, A., and Shrestha, A., 2019. Coccidiosis of Pigs. In: Dubey, J.P. (Ed.) *Coccidiosis in Livestock, Poultry, Companion Animals, and Humans*. (1<sup>st</sup> ed. Vol. 1, pp. 125–145). Taylor & Francis Group, Milton Park. <https://doi.org/10.1201/9780429294105-11>.
- Ketprasit, N., Cheng, I.S., Deutsch, F., Tran, N., Imwong, M., Combes, V., Palasuwan, D., 2020. The characterization of extracellular vesicles-derived microRNAs in Thai malaria patients. *Malar. J.* 19 (1), 285. <https://doi.org/10.1186/s12936-020-03360-z>.
- Khosravi, M., Mirsamadi, E.S., Mirjalali, H., Zali, M.R., 2020. Isolation and functions of extracellular vesicles derived from parasites: The promise of a new era in immunotherapy, vaccination, and diagnosis. *Int. J. Nanomed.* 15, 2957–2969. <https://doi.org/10.2147/IJN.S250993>.
- Koutsogiannis, Z., Mina, J.G., Albus, C.A., Kol, M.A., Holthuis, J.C.M., Pohl, E., Denny, P. W., 2023. *Toxoplasma* ceramide synthases: Gene duplication, functional divergence, and roles in parasite fitness. *FASEB J.* 37 (11), e23229. <https://doi.org/10.1096/fj.2022011603RRR>.
- Leitherer, S., Clos, J., Liebler-Tenorio, E.M., Schleicher, U., Bogdan, C., Soulat, D., 2017. Characterization of the protein tyrosine phosphatase LmpRL-1 secreted by *Leishmania major* via the exosome pathway. *Infect. Immun.* 85. <https://doi.org/10.1128/iai.00084-17>.
- Leung, K.F., Dacks, J.B., Field, M.C., 2008. Evolution of the multivesicular body ESCRT machinery: retention across the eukaryotic lineage. *Traffic* 9 (10), 1698–1716. <https://doi.org/10.1111/j.1600-0854.2008.00797.x>.
- Liangsupree, T., Multia, E., Riekkola, M.L., 2021. Modern isolation and separation techniques for extracellular vesicles. *J. Chromatogr. A* 1636, 461773. <https://doi.org/10.1016/j.chroma.2020.461773>.
- Lindsay, D.S., 2019. *Cystoisospora* species insights from development *in vitro*. *Front. Vet. Sci.* 5, 335. <https://doi.org/10.2307/3279560>.
- Lindsay, D.S., Houk, A.E., Mitchell, S.M., Dubey, J.P., 2014. Developmental biology of *Cystoisospora* (Apicomplexa: Sarcocystidae) monozoic tissue cysts. *J. Parasitol.* 100, 392–398. <https://doi.org/10.1645/13-494.1>.
- Llorente, A., Skotland, T., Sylvänne, T., Kauhainen, D., Róg, T., Orłowski, A., Vattulainen, I., Ekroos, K., Sandvig, K., 2013. Molecular lipidomics of exosomes released by PC-3 prostate cancer cells. *BBA* 1831, 1302–1309. <https://doi.org/10.1016/j.bbalip.2013.04.011>.
- Lv, Q., Li, J., Gong, P., Xing, S., Zhang, X., 2010. *Neospora caninum*: *In vitro* culture of tachyzoites in MCF-7 human breast carcinoma cells. *Exp. Parasitol.* 126, 536–539. <https://doi.org/10.1016/j.exppara.2010.06.006>.
- Mantel, P.-Y., Marti, M., 2014. The role of extracellular vesicles in *Plasmodium* and other apicomplexan parasites. *Cell. Microbiol.* 16 (3), 344–354. <https://doi.org/10.1111/cmi.12257>.
- Matos, G.S., Fernandes, C.M., Del Poeta, M., 2023. Role of sphingolipids in the host-pathogen interaction. *Biochim. Biophys. Acta Mol. Cell Biol. Lipids* 1868 (11), 159384. <https://doi.org/10.1016/j.bbalip.2023.159384>.
- Marcilla, A., Martín-Jaular, L., Trelis, M., de Menezes-Neto, A., Osuna, A., Bernal, D., Fernandez-Becerra, C., Almeida, I.C., Del Portillo, H.A., 2014. Extracellular vesicles in parasitic diseases. *J Extracell Vesicles* 3, 25040. <https://doi.org/10.3402/jev.v3.25040>.
- Matuschka, F., Heydorn, A.O., 1980. Die Entwicklung von *Isoospora suis* Biester und Murray 1934 (Sporozoa:Coccidia:Eimeriidae) im Schwein. *Zool Beitr* 26, 405–476.
- Mayr, A.L., Hummel, K., Leitsch, D., Razzazi-Fazeli, E., 2024. A comparison of bottom-up proteomic sample preparation methods for the human parasite *Trichomonas vaginalis*. *ACS Omega* 9 (8), 0782–0791. <https://doi.org/10.1021/acsomega.3c10040>.
- Mazumdar, J., Striepen, B., Drive, D.W.B., 2007. Make it or take it: fatty acid metabolism of apicomplexan parasites. *Eukaryot. Cell* 6, 1727–1735. <https://doi.org/10.1128/EC.00255-07>.
- Mehdiani, A., Maier, A., Pinto, A., Barth, M., Akhyari, P., Lichtenberg, A., 2015. An innovative method for exosome quantification and size measurement. *J. Vis. Exp.* 17 (95), 50974. <https://doi.org/10.3791/50974>.
- Mihály, J., Deák, R., Szigyártó, I.C., Bóta, A., Beke-Somfai, T., Varga, Z., 2017. Characterization of extracellular vesicles by IR spectroscopy: Fast and simple

- classification based on amide and C\H stretching vibrations. *BBA – Biomembr* 1859, 459–466. <https://doi.org/10.1016/j.bbmem.2016.12.005>.
- Montaner, S., Galiano, A., Trellis, M., Martín-Jaular, L., Del Portillo, H.A., Bernal, D., Marcilla, A., 2014. The role of extracellular vesicles in modulating the host immune response during parasitic infections. *Front. Immunol.* 5, 433. <https://doi.org/10.3389/fimmu.2014.00433>.
- Nawaz, M., Malik, M.I., Hameed, M., Zhou, J., 2019. Research progress on the composition and function of parasite-derived exosomes. *Acta Trop.* 196, 30–36. <https://doi.org/10.1016/j.actatropica.2019.05.004>.
- Nik, M.K., Shahidan, W.N.S., 2020. Non-exosomal and exosomal circulatory microRNAs: which are more valid as biomarkers? *Front. Pharmacol.* 10, 1500. <https://doi.org/10.3389/fphar.2019.01500>.
- Nyonda, M.A., Kloehn, J., Sosnowski, P., Krishnan, A., Lentini, G., Maco, B., Marq, J.B., Hannich, J.T., Hopfgartner, G., Soldati-Favre, D., 2022. Ceramide biosynthesis is critical for establishment of the intracellular niche of *Toxoplasma gondii*. *Cell Rep.* 40 (7), 111224. <https://doi.org/10.1016/j.celrep.2022.111224>.
- Ofir-Birin, Y., Regev-Rudzki, N., 2019. Extracellular vesicles in parasite survival. *Science* 22363 (6429), 817–818. <https://doi.org/10.1126/science.aau4666>.
- Olajide, J.S., Cai, J., 2020. Perils and promises of pathogenic protozoan extracellular vesicles. *Front. Cell. Infect. Microbiol.* 10, 371. <https://doi.org/10.3389/fcimb.2020.00371>.
- Smith, T.G., Walliker, D., Ranford-Cartwright, L.C., 2002a. Sexual differentiation and sex determination in the Apicomplexa. *Trends Parasitol.* 18 (7), 315–323. [https://doi.org/10.1016/s1471-4922\(02\)02292-4](https://doi.org/10.1016/s1471-4922(02)02292-4).
- Tsugawa, H., Cajka, T., Kind, T., Ma, Y., Higgins, B., Ikeda, K., Kanazawa, M., Vander Gheynst, J., Fiehn, O., Arita, M., 2015. MS-DIAL: data-independent MS/MS deconvolution for comprehensive metabolome analysis. *Nat. Methods* 12 (6), 523–526. <https://doi.org/10.1038/nmeth.3393>.
- Omrani, M., Beyrampour, H., Rana, B., Esfahlan, J., Talebi, M., Raesis, M., Serej, Z.A., Akbar-Gharalari, N., Khodakarimi, S., Wu, J., Ebrahimi-Kalan, A., 2023. Global trend in exosome isolation and application: an update concept in management of diseases. *Mol. Cell. Biochem.* 479 (3), 679–691. <https://doi.org/10.1007/s11010-023-04756-6>.
- Pendiuk Goncalves, J., Walker, S.A., Díaz, A., de León, J.S., Yang, Y., Davidovich, I., Busatto, S., Sarkaria, J., Talmon, Y., Borges, C.R., Wolfram, J., 2023. Glycan node analysis detects varying glycosaminoglycan levels in melanoma-derived extracellular vesicles. *Int. J. Mol. Sci.* 24 (10), 8506. <https://doi.org/10.3390/ijms24108506>.
- Pinckney, R.D., Lindsay, D.S., Toivio-Kinnucan, M.A., Blagburn, B.L., 1993. Ultrastructure of *Isospora suis* during excystation and attempts to demonstrate extraintestinal stages in mice. *Vet. Parasitol.* 47, 225–233. [https://doi.org/10.1016/0304-4017\(93\)90024-H](https://doi.org/10.1016/0304-4017(93)90024-H).
- Quairim, T.M., Maia, M.M., da Cruz, A.B., Taniwaki, N.N., Namiyama, G.M., Pereira-Chiocola, V.L., 2021. Characterization of extracellular vesicles isolated from types I, II and III strains of *Toxoplasma gondii*. *Acta Trop.* 219, 105915. <https://doi.org/10.1016/j.actatropica.2021.105915>.
- Ramírez-Flores, C.J., Cruz-Mirón, R., Mondragón-Castelán, M.E., González-Pozos, S., Ríos-Castro, E., Mondragón-Flores, R., 2019. Proteomic and structural characterization of self-assembled vesicles from excretion/secretion products of *Toxoplasma gondii*. *J. Proteomics* 208, 103490. <https://doi.org/10.1016/j.jprot.2019.103490>.
- Raposo, G., Stoorvogel, W., 2013. Extracellular vesicles: Exosomes, ectosomes, and friends. *J. Cell Biol.* 200, 373–383. <https://doi.org/10.1083/jcb.201211138>.
- Scholtyssek, E., Hammond, D.M., 1970. Electron microscope studies of macrogametes and fertilization in *Eimeria bovis*. *Zeitschrift Für Parasitenkd* 34, 310–318. <https://doi.org/10.1007/BF00260299>.
- Shanmugasundaram, A., Gonzalez-Galarza, F.F., Wastling, J.M., Vasieva, O., Jones, A.R., 2013. Library of apicomplexan metabolic pathways: a manually curated database for metabolic pathways of apicomplexan parasites. *Nucleic Acids Res.* 41 (D1), 706–713. <https://doi.org/10.1093/nar/gks1139>.
- Silva, M.S., Faustino, A.M., Mota, M.M., 2019. Unique features of *Toxoplasma gondii* extracellular vesicles and their potential as biomarkers. *Microorganisms* 7 (8), 291. <https://doi.org/10.3390/microorganisms7080291>.
- Skariah, S., McIntyre, M.K., Mordue, D.G., 2010. *Toxoplasma gondii*: determinants of tachyzoite to bradyzoite conversion. *Parasitol. Res.* 107 (2), 253–260. <https://doi.org/10.1007/s00436-010-1899-6>.
- Skotland, T., Sagini, K., Sandvig, K., Llorente, A., 2020. An emerging focus on lipids in extracellular vesicles. *Adv. Drug Deliv. Rev.* 159, 308–321. <https://doi.org/10.1016/j.addr.2020.03.002>.
- Smith, R.C., Vega-Rodríguez, J., Jacobs-Lorena, M., 2014. The *Plasmodium* bottleneck: malaria parasite losses in the mosquito vector. *Mem. Inst. Oswaldo Cruz* 109 (5), 644–661. <https://doi.org/10.1590/0074-0276130597>.
- Smith, T.G., Walliker, D., Ranford-Cartwright, L.C., 2002b. Sexual differentiation and sex determination in the Apicomplexa. *Trends Parasitol.* 18, 315–323. [https://doi.org/10.1016/s1471-4922\(02\)02292-4](https://doi.org/10.1016/s1471-4922(02)02292-4).
- Szempluch, A.J., Sykes, S.E., Hajduk, S.L., 2016. Extracellular vesicle-based communication in parasitic protozoa. *Nature Rev. Microbiol.* 14 (11), 700–713. <https://doi.org/10.1038/nrmicro.2016.134>.
- Théry, C., Witwer, K.W., Aikawa, E., Alcaraz, M.J., Anderson, J.D., Andriantsitohaina, R., Antoniou, A., Arab, T., Archer, F., Atkin-Smith, G.K., Ayre, D.C., Bach, J.M., Bachurski, D., Baharvand, H., Balaj, L., Baldacchino, S., Bauer, N.N., Baxter, A.A., Bebawy, M., Beckham, C., Bedina Zavec, A., Benmoussa, A., Berardi, A.C., Bergese, P., Bielska, E., Blenkiron, C., Bobis-Wozniowicz, S., Boilard, E., Boireau, V., Bongiovanni, A., Borràs, F.E., Bosch, S., Boulanger, C.M., Brakefield, X., Breglio, A.M., Brennan, M.A., Brigstock, D.R., Brisson, A., Broekman, M.L.D., Bromberg, J. F., Bryl-Górecka, P., Buch, S., Buck, A.H., Burger, D., Busatto, S., Buschmann, D., Bussolati, B., Buzás, E.I., Byrd, J.B., Camussi, G., Carter, D.R.F., Caruso, S., Chamley, L.W., Chang, Y.T., Chen, C., Chen, S., Cheng, L., Chin, A.R., Clayton, A., Clerici, S.P., Cocks, A., Cocucci, E., Coffey, R.J., Cordeiro-da-Silva, A., Couch, Y., Coumans, F.A. W., Coyle, B., Crescitelli, R., Criado, M.F., D'Souza-Schorey, C., Das, S., Datta Chaudhuri, A., de Candia, P., De Santana Junior, E.F., De Wever, O., del Portillo, H. A., Demaree, T., Deville, S., Devitt, A., Dhondt, B., Di Vizio, D., Dieterich, L.C., Dolo, V., Dominguez Rubio, A.P., Dominici, M., Dourado, M.R., Driedonks, T.A.P., Duarte, F.V., Duncan, H.M., Eichenberger, R.M., Ekström, K., El Andaloussi, S., Elie-Caille, C., Erdbrügger, U., Falcón-Pérez, J.M., Fatima, F., Fish, J.E., Flores-Bellver, M., Försönits, A., Frelet-Barrand, A., Fricke, F., Fuhrmann, G., Gabriellsson, S., Gámez-Valero, A., Gardiner, C., Gärtner, K., Gaudin, R., Gho, Y.S., Giebel, B., Gilbert, C., Gimona, M., Giusti, I., Goberdhan, D.C.I., Görgens, A., Gorski, S.M., Greening, D.W., Gross, J.C., Gualerzi, A., Gupta, G.N., Gustafson, D., Handberg, A., Haraszti, R.A., Harrison, P., Hegyesi, H., Hendrix, A., Hill, A.F., Hochberg, F.H., Hoffmann, K.F., Holder, B., Holthofer, H., Hosseinkhani, B., Hu, G., Huang, Y., Huber, V., Hunt, S., Ibrahim, A.G., Ikezu, T., Inal, J.M., Isin, M., Ivanova, A., Jackson, H.K., Jacobsen, S., Jay, S.M., Jayachandran, M., Jenster, G., Jiang, L., Johnson, S.M., Jones, J.C., Jong, A., Jovanovic-Talisman, T., Jung, S., Kalluri, R., Kano, S., Kaur, S., Kawamura, Y., Keller, E.T., Khamarri, D., Khomyakova, E., Khvorova, A., Kierulff, P., Kim, K.P., Kislinger, T., Klingeborn, M., Klinke II, D.J., Kornek, M., Kosanović, M.M., Kovács, Á.F., Krämer-Albers, E.M., Krasemann, S., Krause, M., Kurochkin, I.V., Kusuma, G.D., Kuypers, S., Laitinen, S., Langevin, S. M., Languino, L.R., Lannigan, J., Lässer, C., Laurent, L.C., Lavieu, G., Lázaro-Ibáñez, E., Le Lay, S., Lee, M.S., Lee, Y.X.F., Lemos, D.S., Lenassi, M., Leszczynska, A., Li, I.T. S., Liao, Q., Libregts, S.F., Ligeti, E., Lim, R., Lim, S.K., Liné, A., Linnenmannstöns, K., Llorente, A., Lombard, C.A., Lorenowicz, M.J., Lörincz, Á.M., Lötvall, J., Lovett, J., Lowry, M.C., Loyer, X., Lu, Q., Lukomska, B., Lunavat, T.R., Maas, S.L.N., Malhi, H., Marcilla, A., Mariani, J., Mariscal, J., Martens-Uzunova, E.S., Martín-Jaular, L., Martínez, M.C., Martins, V.R., Mathieu, M., Mathivanan, S., Maugeri, M., McGinnis, V.K., McVey, M.J., Meckes Jr, D.G., Meehan, K.L., Mertens, I., Minciacchi, L.R., Möller, A., Møller-Jørgensen, M., Morales-Kastresana, A., Morhayim, J., Mullier, F., Muraca, M., Musante, L., Mussack, V., Muth, D.C., Myburgh, K.H., Najrana, T., Nawaz, M., Nazarenko, I., Nejsum, P., Neri, C., Neri, T., Nieuwland, R., Nimrichter, L., Nolan, J.P., Nolte-T'hoen, E.N.M., Noren Hooten, N., O'Driscoll, L., O'Grady, T., O'Loughlen, A., Ochiya, T., Olivier, M., Ortiz, A., Ortiz, L.A., Osteikoetxea, X., Østergaard, O., Ostrowski, M., Park, J., Pegtel, D.M., Peinado, H., Perut, F., Pfaffl, M.W., Phinney, D.G., Pieters, B.C.H., Pink, R.C., Pisetsky, D.S., Pogge von Strandmann, E., Polakovicova, I., Poon, I.K.H., Powell, B. H., Prada, I., Pulliam, L., Quesenberry, P., Radeghieri, A., Raffai, R.L., Raimondo, S., Rak, J., Ramirez, M.I., Raposo, G., Rayyan, M.S., Regev-Rudzki, N., Ricklefs, F.L., Robbins, P.D., Roberts, D.D., Rodrigues, S.C., Rohde, E., Rome, S., Rouschop, K.M. A., Rughetti, A., Russell, A.E., Saá, P., Sahoo, S., Salas-Huenuleo, E., Sánchez, C., Saugstad, J.A., Saul, M.J., Schiffelers, R.M., Schneider, R., Schøyen, T.H., Scott, A., Shahaj, E., Sharma, S., Shatnyeva, O., Shekari, F., Shelke, G.V., Shetty, A.K., Shiba, K., Siljander, P.R.M., Silva, A.M., Skowronek, A., Snyder II, O.L., Soares, R.P., Sódar, B.W., Soekmadji, C., Sotillo, J., Stahl, P.D., Stoorvogel, W., Stott, S.L., Strasser, E.F., Swift, S., Tahara, H., Tewari, M., Timms, K., Tiwari, S., Tixeira, R., Tkach, M., Toh, W.S., Tomasini, R., Torrecilhas, A.C., Tosar, J.P., Toxavidis, V., Urbanelli, L., Vader, P., van Balkom, B.W.M., van der Grein, S.G., Van Deun, J., van Herwijnen, M.J.C., Van Keuren-Jensen, K., van Niel, G., van Royen, M.E., van Wijnen, A.J., Vasconcelos, M.H., Vechetti Jr, I.J., Veit, T.D., Vella, L.J., Velot, É., Verweij, F.J., Vestad, B., Viñas, J.L., Visnovitz, T., Vukman, K.V., Wahlgren, J., Watson, D.C., Wauben, M.H.M., Weaver, A., Webber, J.P., Weber, V., Wehman, A.M., Weiss, D.J., Welsh, J.A., Wendt, S., Wheelock, Á.M., Wiener, Z., Witte, L., Wolfram, J., Xagorari, A., Xander, P., Xu, J., Yan, X., Yáñez-Mó, M., Yin, H., Yuana, Y., Zappulli, V., Zarubova, J., Žekas, V., Zhang, J.Y., Zhao, Z., Zheng, L., Zheutlin, A.R., Zickler, A. M., Zimmermann, P., Zivkovic, A.M., Zocco, D., Zuba-Surma, E.K., 2018. Minimal information for studies of extracellular vesicles 2018 (MISEV2018): a position statement of the International Society for Extracellular Vesicles and update of the MISEV2014 guidelines. *J. Extracell. Vesicles* 7, 1535750. <https://doi.org/10.1080/20013078.2018.1535750>.
- Toda, H., Diaz-Varela, M., Segui-Barber, J., Roobsoong, W., Baro, B., Garcia-Silva, S., Galiano, A., Gualdrón-López, M., Almeida, A.C.G., Brito, M.A.M., Cardoso de Melo, G., Aparici-Herráiz, I., Castro-Cavadiá, C., Monteiro, W.M., Borrás, E., Sabidó, E., Almeida, I.C., Chojnacki, J., Martínez-Picado, J., Calvo, M., Armengol, P., Carmona-Fonseca, J., Yasnot, M.F., Lauzurica, R., Marcilla, A., Peinado, H., Galinski, M.R., Lacerda, M.V.G., Sattabongkot, J., Fernandez-Becerra, C., Del Portillo, H.A., 2020. Plasma-derived extracellular vesicles from *Plasmodium vivax* patients signal spleen fibroblasts via NF-κB facilitating parasite cytoadherence. *Nat. Commun.* 11, 2761. <https://doi.org/10.1038/s41467-020-16337-y>.
- van Meer, G., Voelker, D.R., Feigenson, G.W., 2008. Membrane lipids: Where they are and how they behave. *Nat. Rev. Mol. Cell Biol.* 9 (2), 112–124. <https://doi.org/10.1038/nrm2330>.
- Walker, R.A., Ferguson, D.J.P., Miller, C.M.D., Smith, N.C., 2013. Sex and *Eimeria*: A molecular perspective. *Parasitology* 140, 1701–1717. <https://doi.org/10.1017/S0031182013000838>.
- Wang, J., Chen, D., Ho, E.A., 2020. Challenges in the development and establishment of exosome-based drug delivery systems. *J. Control. Release* 329, 894–906. <https://doi.org/10.1016/j.jconrel.2020.10.020>.
- Wang, J., Chen, Y.L., Li, Y.K., Chen, D.K., He, J.F., Yao, N., 2021. Functions of Sphingolipids in pathogenesis during host-pathogen interactions. *Front. Microbiol.* 12, 701041. <https://doi.org/10.3389/fmicb.2021.701041>.
- Welsh, J.A., Goberdhan, D.C.I., O'Driscoll, L., Buzas, E.I., Blenkiron, C., Bussolati, B., Cai, H., Di Vizio, D., Driedonks, T.A.P., Erdbrügger, U., Falcon-Perez, J.M., Fu, Q.L., Hill, A.F., Lenassi, M., Lim, S.K., Mahoney, M.G., Mohanty, S., Möller, A.,

- Nieuwland, R., Ochiya, T., Sahoo, S., Torrecilhas, A.C., Zheng, L., Zijlstra, A., Abuelreich, S., Bagabas, R., Bergese, P., Bridges, E.M., Bruciale, M., Burger, D., Carney, R.P., Cocucci, E., Crescitelli, R., Hanser, E., Harris, A.L., Haughey, N.J., Hendrix, A., Ivanov, A.R., Jovanovic-Taliman, T., Kruh-Garcia, N.A., Faustino, V. K., Kyburz, D., Lässer, C., Lennon, K.M., Lötvall, J., Maddox, A.L., Martens-Uzunova, E.S., Mizenko, R.R., Newman, L.A., Ridolfi, A., Rohde, E., Rojalin, T., Rowland, A., Saftics, A., Sandau, U.S., Saugstad, J.A., Shekari, F., Swift, S., Ter-Ovanesyan, D., Tosar, J.P., Useckaite, Z., Valle, F., Varga, Z., van der Pol, E., van Herwijnen, M.J.C., Wauben, M.H.M., Wehman, A.M., Williams, S., Zendrini, A., Zimmerman, A.J. MISEV Consortium, Théry, C., Witwer, K.W., 2022. Minimal information for studies of extracellular vesicles (MISEV2023): From basic to advanced approaches. *J Extracell Vesicles* 13 (2), e12404. <https://doi.org/10.1002/jev2.12404>.
- Welti, R., Mui, E., Sparks, A., Wernimont, S., Isaac, G., Kirisits, M., Roth, M., Roberts, C. W., Botté, C., Maréchal, E., McLeod, R., 2007. Lipidomic analysis of *Toxoplasma gondii* reveals unusual polar lipids. *Biochemistry* 46 (48), 13882–13890. <https://doi.org/10.1021/bi7011993>.
- White, R., Sotillo, J., Ancarola, M.E., Borup, A., Boysen, A.T., Brindley, P.J., Buzás, E.I., Cavallero, S., Chaiyadet, S., Chalmers, I.W., Cucher, M.A., Dagenais, M., Davis, C. N., Devaney, E., Duque-Correa, M.A., Eichenberger, R.M., Fontenla, S., Gasan, T.A., Hokke, C.H., Kosanovic, M., Kuipers, M.E., Laha, T., Loukas, A., Maizels, R.M., Marcilla, A., Mazanec, H., Morphey, R.M., Neophytou, K., Nguyen, L.T., Nolte-t Hoen, E., Povelones, M., Robinson, M.W., Rojas, A., Schabussova, I., Smits, H.H., Sungpradit, S., Tritten, L., Whitehead, B., Zakeri, A., Nejsun, P., Buck, A.H., Hoffmann, K.F., 2023. Special considerations for studies of extracellular vesicles from parasitic helminths: A community-led roadmap to increase rigour and reproducibility. *J Extracell Vesicles* 12 (1), e12298. <https://doi.org/10.1002/jev2.12298>.
- Witwer, K.W., Goberdhan, D.C.I., O'Driscoll, L., Théry, C., Welsh, J.A., Blenkiron, C., Buzás, E.I., Di Vizio, D., Erdbrügger, U., Falcón-Pérez, J.M., Fu, Q.L., Hill, A.F., Lenassi, Lötvall, J., Nieuwland, R., Ochiya, T., Rome, S., Sahoo, S., Zheng, L., 2021. Updating MISEV: Evolving the minimal requirements for studies of extracellular vesicles. *J Extracell Vesicles* 10 (14), e12182. <https://doi.org/10.1002/jev2.12182>.
- Wong, L.W., Mak, S.H., Goh, B.H., Lee, W.L., 2023. The convergence of FTIR and EVs: Emergence strategy for non-invasive cancer markers discovery. *Diagnostics* 13 (1), 22. <https://doi.org/10.3390/diagnostics13010022>.
- Worliczek, H.L., Buggelsheim, M., Saalmüller, A., Joachim, A., 2007. Porcine isosporosis: infection dynamics, pathophysiology and immunology of experimental infections. *Wien. Klin. Wochenschr.* 119, 33–39. <https://doi.org/10.1007/s00508-007-0859-3>.
- Worliczek, H.L., Gerner, W., Joachim, A., Mundt, H.C., Saalmüller, A., 2009. Porcine coccidiosis - investigations on the cellular immune response against *Isospora suis*. *Parasitol. Res.* 105, 151–156. <https://doi.org/10.1007/s00436-009-1506-x>.
- Wowk, P.F., Zardo, M.L., Miot, H.T., Goldenberg, S., Carvalho, P.C., Mörking, P.A., 2017. Proteomic profiling of extracellular vesicles secreted from *Toxoplasma gondii*. *Proteomics* 17, 15–16. <https://doi.org/10.1002/pmic.201600477>.
- Yang, C., Arrizabalaga, G., 2017. The serine/threonine phosphatases of apicomplexan parasites. *Mol. Microbiol.* 106 (1), 1–21. <https://doi.org/10.1111/mmi.13715>.
- Yong, H., Zhao, L., Zhao, H., 2021. Comparative analysis of EV markers in diverse apicomplexans. *Int. J. Parasitol.* 51 (5), 437–448. <https://doi.org/10.1016/j.ijpara.2021.03.004>.
- Zhao, H., Achreja, A., Iessi, E., Logozzi, M., Mizzoni, D., Di Raimo, R., Nagrath, D., Fais, S., 2018. The key role of extracellular vesicles in the metastatic process. *Biochim. Biophys. Acta* 1869 (1), 64–77. <https://doi.org/10.1016/j.bbcan.2017.11.005>.
- Zoia, M., Yesodha Subramanian, B., Eriksson, K.K., Ravi, M.S., Yaghmaei, S., Fellay, I., Scolari, B., Walch, M., Mantel, P.Y., 2022. Validation of effective extracellular vesicles isolation methods adapted to field studies in malaria endemic regions. *Front. Cell Dev. Biol.* 10, 812244. <https://doi.org/10.3389/fcell.2022.812244>.